

Best Available Copy

REPORT SD-TR-80-37

✓

**LEVEL II**

12

ADA 085778

# A Review of the Science and Technology of Cathodes from the Viewpoint of Spacecraft TWT Applications

G. W. STUPIAN  
Chemistry and Physics Laboratory  
Laboratory Operations  
The Aerospace Corporation  
El Segundo, Calif. 90245

1 June 1980

Interim Report

SDTIC  
ELECTE  
JUN 19 1980  
E

APPROVED FOR PUBLIC RELEASE;  
DISTRIBUTION UNLIMITED

Prepared for  
SPACE DIVISION  
AIR FORCE SYSTEMS COMMAND  
Los Angeles Air Force Station  
P.O. Box 92960, Worldway Postal Center  
Los Angeles, Calif. 90009

DDC FILE COPY

80 6 19 051

This interim report was submitted by The Aerospace Corporation, El Segundo, CA 90245, under Contract No. F04701-79-C-0080 with the Space Division, Contracts Management Office, P. O. Box 92960, Worldway Postal Center, Los Angeles, CA 90009. It was reviewed and approved for The Aerospace Corporation by S. Siegel, Director, Chemistry and Physics Laboratory. Gerhard E. Aichinger was the project officer for Mission-Oriented Investigation and Experimentation (MOIE) Programs.

This report has been reviewed by the Public Affairs Office (PAS) and is releasable to the National Technical Information Service (NTIS). At NTIS, it will be available to the general public, including foreign nations.

This technical report has been reviewed and is approved for publication. Publication of this report does not constitute Air Force approval of the report's findings or conclusions. It is published only for the exchange and stimulation of ideas.



Gerhard E. Aichinger  
Project Officer

FOR THE COMMANDER



Evan R. Brössman, Chief  
Contracts Management Office

UNCLASSIFIED

SECURITY CLASSIFICATION OF THIS PAGE (When Data Entered)

REPORT DOCUMENTATION PAGE		READ INSTRUCTIONS BEFORE COMPLETING FORM
1. REPORT NUMBER SD TR-80-37	2. GOVT ACCESSION NO. AD-A085778	3. RECIPIENT'S CATALOG NUMBER
4. TITLE (and Subtitle) A REVIEW OF THE SCIENCE AND TECHNOLOGY OF CATHODES FROM THE VIEWPOINT OF SPACECRAFT TWT APPLICATIONS,	5. TYPE OF REPORT & PERIOD COVERED Interim rept.	6. PERFORMING ORG. REPORT NUMBER TR-0080(5970-03)-2
7. AUTHOR(s) Gary W. Stupian	8. CONTRACT OR GRANT NUMBER(s) F04701-79-C-0080	
9. PERFORMING ORGANIZATION NAME AND ADDRESS The Aerospace Corporation El Segundo, Calif. 90245	10. PROGRAM ELEMENT, PROJECT, TASK AREA & WORK UNIT NUMBERS 12, 76	
11. CONTROLLING OFFICE NAME AND ADDRESS Space Division Air Force Systems Command Los Angeles, Calif. 90009	12. REPORT DATE 1 June 1980	13. NUMBER OF PAGES 72
14. MONITORING AGENCY NAME & ADDRESS (if different from Controlling Office)	15. SECURITY CLASS. (of this report) Unclassified	15a. DECLASSIFICATION/DOWNGRADING SCHEDULE
16. DISTRIBUTION STATEMENT (of this Report)  Approved for public release; distribution unlimited		
17. DISTRIBUTION STATEMENT (of the abstract entered in Block 20, if different from Report)		
18. SUPPLEMENTARY NOTES		
19. KEY WORDS (Continue on reverse side if necessary and identify by block number)  Thermionic Cathodes Thermionic Emission Traveling Wave Tubes		
20. ABSTRACT (Continue on reverse side if necessary and identify by block number)  The current state of the art of cathode science and technology is summarized, with emphasis on the types of cathode now used, or with potential use, in U.S. Air Force communication satellites. The intent is that this report be a stand-alone discussion of cathode construction and of the basic physics of electron emission. Emphasis is placed on thermionic cathodes; however, one nonthermionic emitter, the field emitter, is discussed briefly. For the thermionic emitters, the barium (calcium and strontium) oxide cathode and		

DD FORM 1473  
(FACSIMILE)UNCLASSIFIED 409382  
SECURITY CLASSIFICATION OF THIS PAGE (When Data Entered)

## 19. KEY WORDS (Continue /)

## 20. ABSTRACT (Continued)

dispenser cathodes (based on barium) are discussed, along with variant types of the oxide and dispenser cathodes. Thorium-based cathodes and lanthanum hexaboride cathodes are also described. Some of the available data on cathode failure modes and cathode lifetime are included. Electron emission from solids has been studied with varying intensity since the last century, and the present discussion, because of the scope of the subject, of course is incomplete. Extensive literature references are given, however.

It has been concluded that dispenser-impregnated cathodes will have to be employed to meet future U.S. Air Force (SD) mission requirements. Of these cathodes, the impregnated Type B and osmium-coated Type M cathodes offer the highest probability of success. There is no fundamental reason why more exotic emitters, e.g., field emitters, could not ultimately be employed in space applications. However, the difficulty in acquiring sufficient test data in any reasonable time to flight-qualify components based on a new technology is so great that impregnated cathodes will almost certainly be utilized.

It is also concluded that studies of impregnated cathodes in which modern surface analysis techniques are used for submicron surface elemental analysis, especially if used in conjunction with techniques for mapping cathode work functions with high spatial resolution, would be very valuable and should ultimately permit identification of specific cathode failure mechanisms. Application of this information could result in a marked improvement in cathode reliability.

Accession For	
NTIS GRA&I	<input checked="" type="checkbox"/>
DDC TAB	<input type="checkbox"/>
Unannounced	<input type="checkbox"/>
Justification	
By _____	
Distributor/	
Availability Codes	
Dist	Avail and/or special
A	

## CONTENTS

I.	INTRODUCTION . . . . .	5
II.	FUNDAMENTAL CONCEPTS OF THERMIONIC EMISSION . . . . .	7
	A. Emission Equations . . . . .	7
	B. Cathode Design Strategy . . . . .	12
III.	ALKALINE EARTH OXIDE CATHODES . . . . .	15
	A. Construction . . . . .	15
	B. Principles of Oxide Cathode Operation . . . . .	16
IV.	BARIUM MONOLAYER CATHODES . . . . .	23
	A. Construction . . . . .	24
	B. Principles of Operation of Barium Monolayer Cathodes . . . . .	27
V.	OTHER MONOLAYER CATHODES . . . . .	39
	A. Thoriated Tungsten Cathodes . . . . .	39
	B. Lanthanum Hexaboride Cathodes . . . . .	40
VI.	TEST PROCEDURES AND LIFE-TEST DATA FOR THERMIONIC CATHODES . . . . .	41
VII.	FIELD-EMISSION CATHODES . . . . .	45
VIII.	CONCLUSIONS . . . . .	47
	REFERENCES . . . . .	49
	APPENDIXES: A. EMISSION EQUATIONS . . . . .	53
	B. WORK FUNCTION . . . . .	67

*page 2 blank*

FIGURES

1.	Energy-Level Diagrams for a Metal and for a Semiconductor . .	8
2.	Parallel Plate Diode . . . . .	11
3.	Energy-Level Diagrams for Band Bending in n-Type Semiconductor . . . . .	20
4.	L-Dispenser Cathode . . . . .	25
5.	Impregnated Cathode . . . . .	26
6.	Potential Energy Diagrams Illustrating Additional Work-Function Lowering Obtained with Monolayer Cathode as Result of Increasing Substrate Work Function . . . . .	35
7.	Stanford Research Institute Field-Emission Cathode . . . . .	46
A-1.	a. Energy-Level Diagram for Metal and Corresponding Density of Electron States. b. At $T = 0$ K. c. At $T > 0$ K. . . . .	54
A-2.	Electron Energy as Function of Distance from Surface of Metal in Absence of Applied Field . . . . .	59
A-3.	Electrostatic Potential as Function of Distance from Surface in Presence of Externally Applied Electric Field. . . . .	61
B-1.	Electron Double Layer Formation at Metal Surface as Result of Spreading of the Electron Distribution . . . . .	68
B-2.	General Behavior of Work Function as Function of Surface Coverage for Alkali or Alkaline Earth Element Absorbed on Metal Substrate . . . . .	72
B-3.	Potential Energy Diagrams . . . . .	74

PRECEDING PAGE BLANK-NOT FILMED

## I. INTRODUCTION

The success of U. S. Air Force communications satellite missions depends upon the availability of traveling wave tubes (TWTs) capable of delivering adequate microwave power for extended periods.<sup>1</sup> Traveling wave tubes will, not in the near future, be replaced by solid-state devices as high-power microwave amplifiers in frequency bands of interest to the Air Force. The satisfactory performance of a TWT is dependent upon the proper functioning of a thermionic cathode.

It is not certain that cathodes capable of delivering adequate current densities with lifetimes necessary to meet SD mission requirements can be produced with the present manufacturing technology. The production of adequate cathodes for extended space missions is probably one of the greatest technological challenges in Air Force satellite programs. In view of the considerable amount of work devoted to the study of cathodes during the era of ascendancy of the vacuum tube, it has been widely assumed that the fabrication of cathodes suitable for use in space-qualified TWTs presents no extraordinary problems. This assumption is invalid. Tubes in ground or airborne applications generally can be replaced on a schedule or as necessary. A lifetime of some thousands of hours was and is often adequate. The success or failure of a modern communications satellite still hinges upon the performance of cathodes developed for use under much less exacting conditions.

Various aspects of the cathode problem have been treated in several published reviews.<sup>3-7</sup> Basic and applied results particularly relevant to the utilization of cathodes in space applications have been compiled in this report. This document is intended to be a stand-alone discussion of cathodes, including fundamental considerations of electron emission and practical considerations of cathode construction and failure. The literature in the field is so extensive that no attempt can be made to cover every aspect of cathode science and technology in exhaustive detail. It is hoped that the selection of topics and

the emphasis chosen will make the document useful to those wishing to acquire some understanding of the spacecraft cathode problem. In addition, extensive literature references are included.

The emphasis in this report is on thermionic emission simply because thermionic cathodes have been predominant in tube technology to date, but one other type of cathode with potential space applications, the field emitter, is treated briefly. Basic equations governing thermionic emission that are fundamental to any description of cathode operation are given. The various types of thermionic cathodes then are described. There are many different kinds of thermionic cathodes, and some logical means of classification is essential to an orderly presentation. Cathodes now used in TWTs fall into two general categories: alkaline earth oxide cathodes and barium monolayer cathodes. These cathodes and their variants are dealt with in Sections III and IV. Monolayer cathodes other than those based on barium are discussed in Section V. Thermionic-emitter life-test data are presented in Section VI. Field-emission cathodes are discussed in Section VII. Conclusions and recommendations regarding steps necessary to ensure the future availability of cathodes capable of meeting Air Force satellite requirements are presented in Section VIII. More detailed discussions of the emission equations and of the concept of the work function are included in the appendixes.

In recent years, modern techniques for surface analysis, e.g., x-ray photoelectron spectroscopy, Auger electron spectroscopy, and ion microprobe analysis, have been developed; they make possible detailed studies of cathodes not previously feasible. Most of the earlier work on cathodes predated these experimental advances. Although the modern techniques are now beginning to be applied to the problem, much work on the characterization of cathode surfaces remains to be done. As much of the newer work as possible is included in this review.

## II. FUNDAMENTAL CONCEPTS OF THERMIONIC EMISSION

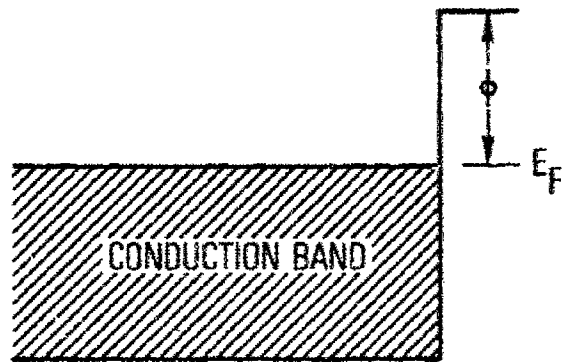
Vacuum-tube technology is based on the manipulation of streams of electrons by electric and magnetic fields. The electron source is the cathode. Cathodes used in vacuum tubes are usually thermionic, i.e., electrons are "boiled off" by raising the temperature; however, cathodes based on other emission processes, e.g., photoemission and secondary emission, have been employed in specialized applications. The study of thermionic emission has a long history. The escape of electrons from hot filaments was first observed by Edison, and the still used alkaline earth oxide cathode was invented by Wehnelt in 1903. Considerable effort was devoted to studies of thermionic emission until the late 1950s when the rise of the transistor curtailed the interest in vacuum tubes and in research directly or indirectly related to vacuum tubes. During the 1960s, there was some renewed interest in thermionic emission for direct conversion of heat to electrical energy, but, for the most part, thermionic emission has been neglected in recent years.<sup>8</sup>

Thermionic emission is analogous to the evaporation of molecules from a liquid. In both cases, particles must be given sufficient thermal energy to escape from the emitting medium. For an evaporating liquid, the necessary energy is called the heat of vaporization. For thermionic emission, the energy barrier is called the work function and is defined as the energy required to remove an electron at the Fermi level to an infinite distance. The relation of the work function to the energy band structure of solids is illustrated for a metal and for a semiconductor in Figs. 1a and 1b, respectively. The work function is a measurable quantity and plays a key role in understanding the thermionic emission process.

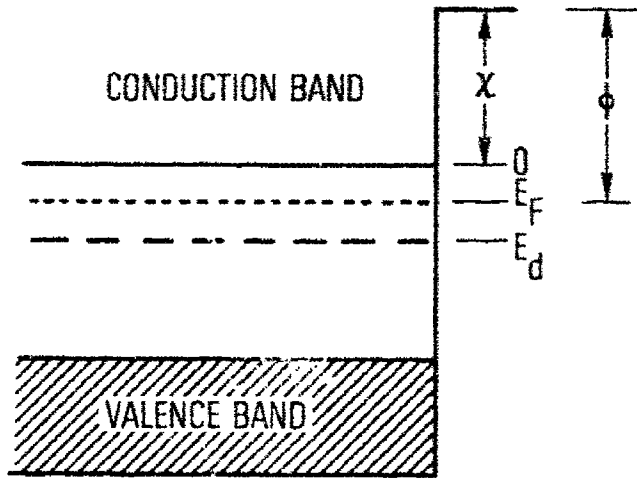
### A. EMISSION EQUATIONS

#### 1. TEMPERATURE-LIMITED EMISSION

The electron current emitted from a surface at temperature  $T(K)$  depends on the value of the work function  $\phi$  and, ideally, is given by the Richardson-Dushman equation



a.



b.

Fig. 1. Energy-Level Diagrams. a. Metal.  
 b. n-type semiconductor.  $E_F$  and  $E_D$  are the Fermi energy and donor level energy, respectively, measured from the bottom of the conduction band.

$$J = AT^2 e^{-\phi/kT} \quad (1a)$$

where J is the electron current density in amperes per square centimeter.<sup>5</sup> The universal (thermionic) Richardson constant A is

$$A = \frac{4\pi m e k^2}{h^3} = 120 \text{ A/cm}^2 \text{K}^2 \quad (1b)$$

A derivation of the Richardson-Dushman equation is given in Appendix A. The Richardson-Dushman equation can be derived with the use of very general thermodynamic arguments that are essentially independent of the energy-band structure of the emitter. Equation (1a) is therefore valid for all types of emitters with suitable slight modifications. An example of such a minor modification arises because electrons may, instead of being emitted, undergo Bragg reflection back into the bulk. A reflection coefficient  $\bar{r}$  is introduced to account for this phenomenon, and Equation (1a) can be rewritten:

$$J = A(1 - \bar{r})T^2 e^{-\phi/kT} \quad (2)$$

The work function depends on both the bulk band structure and on the surface dipole layers brought about by surface crystallographic structure and by the presence of ionizable surface species. It is customary to attempt to fit emission data from many different types of thermionic cathodes with an expression of the form of Eq. (2), although a plot of  $\ln J/T^2$  versus  $1/T$  does not always yield a straight line over a wide temperature range (for reasons to be discussed later). However, with the use of the proper expression for  $\phi$ , Eq. (2) is a useful starting point in describing thermionic emission from a variety of emitters.

Equation (2) yields the maximum emission current density that can be obtained from a cathode with a given work function at temperature T and

describes the situation known as temperature-limited emission. Another electrode (the anode) is used to collect the emitted electrons in order to actually measure the electron emission current from a cathode. For sufficiently high positive anode voltages, the emission current is indeed dependent only on temperature and not upon anode voltage.

## 2. SPACE-CHARGE-LIMITED EMISSION

The cathode in a TWT cannot be operated in the temperature-limited region because under such conditions small changes in temperature result in substantial changes in emission current. For example, for a cathode with a work function of 1.8 eV operating at 1100 C,  $(1/J)(\partial J/\partial T) \approx 1.3\%/K$ . Stable tube operation is difficult to achieve when slight changes in cathode temperature cause such changes in emission current. Traveling wave tubes are operated in a space-charge-limited mode to minimize this possible instability, i. e., anode voltage for a particular cathode temperature is kept sufficiently low to ensure that a charge cloud is maintained in front of the cathode. The charge cloud rather than the cathode itself may be viewed as the emitter. With a simple diode geometry with planar anode and cathode assumed (Fig. 2), the current-voltage relationship for the space-charge region is easily derived by solving the Poisson equation to yield

$$J = \frac{4\epsilon_0}{9} \sqrt{\frac{2e}{m}} \frac{1}{L^2} V^{3/2} \quad (3)$$

where  $L$  is the cathode to anode spacing, and the other symbols have their usual meanings. This expression is known as the Langmuir-Child law. It is necessary that  $\phi/T$  be small enough that the emission current, as given by the Richardson-Dushman equation, can sustain the space-charge cloud in order for a cathode to evidence the behavior described by the Langmuir-Child law. The Langmuir-Child law is discussed in more detail in Appendix A.

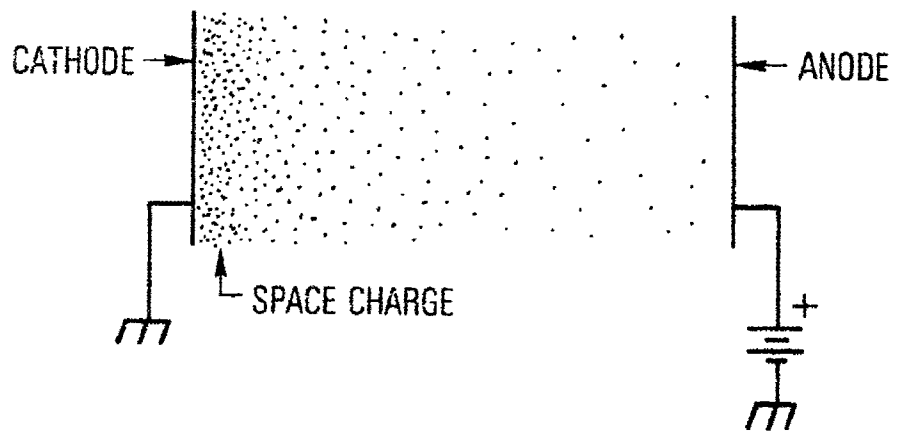


Fig. 2. Parallel Plate Diode

### 3. PATCH EFFECTS

In the derivation of the Richardson-Dushman equation, it is assumed that the work function of a surface is uniform, which is not the situation prevailing for a practical cathode. The surface of a real cathode consists of "patches" of differing work functions. The effect of cathode inhomogeneities depends upon the emission region in which the cathode is being operated. A cathode in a diode test configuration that is operated in the space-charge region is considered. Cathode current is practically independent of the cathode work function since emitted electrons are essentially drawn from the space-charge cloud. As the anode voltage becomes more positive, the higher work function patches reach saturation, i. e., emission is described by the Richardson-Dushman equation, and the slope of the  $J$  versus  $V$  curve decreases. Eventually, all patches will contribute a saturated emission current, governed by individual work functions, to the total current. A Richardson plot,  $\ln J/T^2$  versus  $1/T$ , will yield an "effective work function" and an "effective Richardson constant." These quantities can be related to parameters characteristic of the patch distribution.<sup>9</sup> Patches are directly observable with the use of several different experimental techniques.<sup>10</sup>

#### B. CATHODE DESIGN STRATEGY

Even though traveling wave tubes are operated in the space-charge-limited region, Eq. (2) is still of primary importance since it governs electron density in the space-charge cloud. The product of the work function and the emission current represents power that must be supplied to the cathode to sustain emission (in addition to radiative and conductive heat losses). A lower work function, and thus for a given emission current, a lower operating temperature implies more stable cathode operation in general and a longer operating lifetime as well as improved thermal efficiency. Thus, all practical thermionic cathode designs have as a basis the preparation of surfaces with the lowest possible work function and the highest possible emitting area.

There are, however, additional constraints on cathode design and fabrication. For example, the melting point of the cathode material must be sufficiently high to ensure structural integrity at the operating temperature. For some terrestrial applications, resistance to air exposure (when cold) or to occasional ion bombardment by residual tube gases as a result of accidental glow discharge is essential. Current density requirements also vary. Mechanical stability is particularly important for TWT applications because of focusing requirements.

Pure metals and alloys, semiconductor materials, and systems consisting of work-function-lowering surface dipole layers on metallic substrates have all been used as thermionic emitters for various applications. Of the pure metals, only tungsten, rhenium, and tantalum have sufficiently high melting temperatures to yield significant emission current densities. For tungsten,  $J \approx 300 \text{ mA/cm}^2$  at 2500 K, and the thermal efficiency is roughly 4 to 20 mA/W.<sup>11</sup> Required operating temperatures and attainable efficiencies are not satisfactory for spacecraft TWT applications. Thus, in the following discussion of "practical" thermionic emitters, the alkaline earth oxide and dispenser cathodes (semiconductor and monolayer, respectively) will be emphasized since these cathodes and their variant types play a dominant role in meeting the high-current density requirements of spacecraft TWT operation.

### III. ALKALINE EARTH OXIDE CATHODES

The alkaline earth oxide cathode has been in general use for many years and is widely employed in traveling wave tubes. Current densities of  $300 \text{ mA/cm}^2$  are attained at about  $750^\circ\text{C}$ . However, operation at higher temperatures seriously degrades cathode life and stability. Thus, although alkaline earth oxide cathodes should meet some present Air Force mission requirements, projected demands for current densities of  $1 \text{ amp/cm}^2$  for 7 to 10 years on orbit will ultimately mean that other cathode types will have to be considered for use. The oxide cathodes are described in this section, and some possible types of cathodes for future applications are discussed.

#### A. CONSTRUCTION

The alkaline earth oxide cathode consists of a layer of BaO, SrO, and CaO on a nickel support. The alkaline earths are initially deposited as a slurry of the carbonates with an organic binder. A typical mixture of ingredients results in a final product with a 5/3/2 molar ratio of Ba/Sr/Ca. The carbonate mixture is heated in vacuum to  $900$  to  $1150^\circ\text{C}$  to decompose the carbonates to the oxides. The final oxide thickness is typically approximately  $50 \mu\text{m}$ .

Immediately after carbonate decomposition, the cathode exhibits low emission and low conductivity. For efficient operation, the cathode must be activated. The nature of the actual processes occurring upon activation is a matter of contention. Certain reducing elements or "activators" in the nickel substrate apparently play a vital role in the activation process. These elements, carbon, zirconium, magnesium, manganese, aluminum, silicon, and, perhaps, tungsten, were originally added to the nickel to promote workability, not to enhance cathode emission.

Several variants of the oxide cathode are in use, including the molded nickel,<sup>12</sup> Medicus,<sup>13</sup> and coated powder cathodes.<sup>14</sup> One could argue whether some of these cathodes might perhaps be better classified as variants of the dispenser cathode (Section IV); some might also logically be termed intermediate between oxide and dispenser types.

In all of these variants of the oxide cathode, nickel powder in different concentrations, sometimes with an activator, e.g.,  $ZrH_2$ , is mixed with the alkaline earth oxides. Various advantages are claimed for these cathodes, and various rationales have been presented to explain the improved performance. These claimed improvements usually include not only higher current density for a given operating temperature but often easier control of the shape of the cathode surface and increased resistance to poisoning. In the molded nickel cathode, the cathode coating is 69 wt% Ni powder, 30% alkali carbonates, and 1% activator.<sup>12</sup> In the Medicus cathode, the coating is approximately 75 wt% Ni.<sup>13</sup>

The coated powder cathode (CPC), in contrast, contains only 0.5 to 3.0 wt% Ni. A rationale for the performance of this cathode has been developed<sup>14</sup> and is presented below. The nickel network can evaporate during operation and must be replaced with nickel from the cathode base; otherwise, the CPC becomes a conventional oxide cathode. Further details of fabrication techniques for these different cathodes can be found in the references cited.

## B. PRINCIPLES OF OXIDE CATHODE OPERATION

### 1. GENERAL COMMENTS

A high thermionic-emission current is generally associated with a high electron-energy density in the conduction band of the emitter and with as small a work function as possible. In addition, the bulk electrical resistivity of the emitter should be low in order to eliminate excessive voltage drops that could cause undesired heating or spark discharges. These conditions may be

satisfied by metals or by n-type semiconductors (Appendix A). The large electronegativity difference between barium and oxygen implies that BaO (and similarly, other alkaline earth oxides) would be highly ionic and good electrical insulators. However, because of the doping that inevitably occurs during cathode fabrication and activation, the oxide cathode material is, in fact, an n-type semiconductor.

Any consistent theory explaining the mechanism of emission from the oxide cathode requires an understanding of the origin of the donor levels responsible for semiconducting behavior, and much experimental and theoretical work has been directed toward this end. A theory must also account for certain experimental observations about oxide cathodes. These observations include the necessity for activation mentioned earlier, the fact that temperatures derived from current-voltage plots (Boltzmann temperatures) may disagree with pyrometric temperatures,<sup>15</sup> and the susceptibility of oxide cathodes to poisoning by adsorbed electronegative species. A theory must also explain the pulse behavior of oxide cathodes. Although an oxide cathode can deliver only a few hundred milliamperes per square centimeter under steady-state conditions, current up to  $100 \text{ A/cm}^2$  can be obtained for times on the order of 10 msec by pulsing the anode voltage.

## 2. NATURE OF THE DONOR LEVELS

The identification of the donor levels in the oxide cathode is a difficult problem, and the issue has still not been finally resolved. Whatever the nature of the donor levels, the donor concentration in a cathode is a complex function not only of processes internal to the cathode but of the interaction of the cathode with the ambient tube environment. The cathode may be considered a reducing agent and the remainder of the tube an oxidizing agent. An activated cathode is intrinsically reactive, and chemical species originating anywhere in the tube that are capable of reaching the cathode may affect it. A fairly complete treatment of the various dynamic equilibria in an oxide cathode has been presented by Tischer,<sup>16</sup> who considered simultaneous equilibria between oxygen

vacancies and F centers, between oxygen in the oxide and ambient gaseous oxygen, and between gaseous oxygen and BaO.

Many investigators have given importance to the role of "excess barium," i. e., barium in excess of the stoichiometric requirement for BaO, in accounting for donor levels. Excess barium presumably in some way activates the cathode through the formation of surface states. The excess barium concept does not immediately explain the accompanying increase in electrical conductivity in the activated cathode, since the barium excess is small (this difficulty may be circumvented for barium segregated at grain surfaces, especially for small grains where surface effects influence much of the total BaO volume). Nergaard identified the actual donors in BaO as F centers, i. e., an oxygen vacancy occupied by an electron.<sup>17</sup> The electrons come from the barium atoms. When current is drawn from the cathode, barium ions should drift away from the surface region into the bulk, and the pulse and anomalous Schottky behavior of the cathode would be explained. The Nergaard donor picture also provides a convenient explanation for the beneficial effect of added nickel in the coated powder cathode. The nickel presumably coats the (Ba, Sr)O grains, prevents the growth of large, inactive crystals, and provides conducting paths through the oxide. As a consequence of these conducting paths, the electric field resulting from the applied anode voltage has a large component transverse rather than perpendicular to the surface. Donors are retained in the surface region and emission is facilitated.<sup>14</sup>

On the other hand, Plumlee concluded that the amount of excess barium in BaO is insufficient to account for the necessary donor density.<sup>18</sup> This conclusion was based on measurements of the barium vapor pressure over BaO, chemical determination of excess barium, and lack of correlation between electron emission and measured barium excess in cathodes. Plumlee proposed that the donor centers were  $\text{OH}^-$  ions on the basis of chemical intuition combined with mass spectrometer measurements.

### 3. THEORIES OF THE OXIDE CATHODE

Other aspects of cathode structure, in addition to the various concepts concerning the nature of the donor levels presented in Section III. B. 2, have to be invoked to more fully explain cathode function.

Chin et al. report that the grain structure of the cathode plays a central role.<sup>19</sup> Barium ions adsorbed on the grain surfaces (both surfaces internal to the cathode structure and external surfaces) cause band bending (Fig. 3) that both lowers the work function and increases conductivity in the surface region. Since the cathode grains are small, the perturbed region constitutes an appreciable fraction of the cathode volume, and the bulk conductivity is substantially affected. The correlation between electron emission and conductivity thus is understandable.

The observed electrical conductivity of oxide cathodes over a wide temperature range (600 to 1250 K) is best explained by the combination of two mechanisms.<sup>20</sup> At low temperatures, current flow is along paths from grain to grain. At high temperature ( $\geq 800$  K), the electron gas in the intergranular spaces is sufficiently dense that "pore conduction" by the electron gas is dominant. This pore conduction model is supported experimentally by (1) the observation that the high-temperature conductivity is suppressed by xenon gas at a pressure of 25 atm,<sup>21</sup> and (2) the observation that electrical conductivity is not affected by a magnetic field below 800 K but decreases with applied magnetic field above 800 K.<sup>22</sup> The pore conduction model for electrical conductivity was combined with a single-crystal donor model for thermionic emission in Surplice's "unified" theory of the oxide cathode.<sup>22</sup> The cathode is considered to be composed of small grains in which surface effects dominate bulk effects. Surplice attributes the low cathode work function to band bending produced by surface states formed by adsorption of

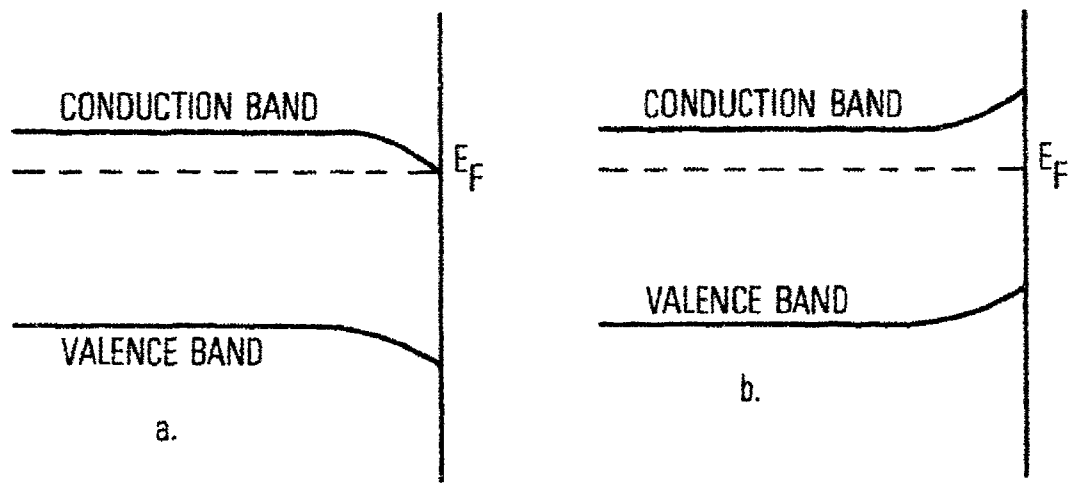
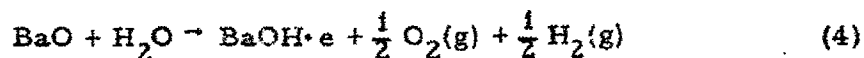


Fig. 3. Energy-Level Diagrams for Band Bending in n-Type Semiconductor. a. Effect of ionized surface donors. b. Effect of ionized surface acceptors.

various residual gas species. One such adsorption process (as proposed by Plumlee)<sup>18</sup> is



where the BaOH·e species acts as a surface electron trap with a long lifetime.

Conducting "filaments" consisting of chains of metal atoms separated by oxygen vacancies within the bulk oxide have been proposed by Dearnally as an alternative explanation of various properties of oxide cathodes.<sup>23</sup> Oxygen is removed, at the activation temperature, by reducing agents present in the oxide coating. The oxide may become locally conductive at certain points at the metal-metal oxide interface through aggregation of vacancies. It is postulated that metal-rich filaments then form under the influence of the electric field usually applied during activation and grow through the coating. In Dearnally's view, emission from an oxide cathode is localized at the filament ends and really represents emission from a metal. The high-emission current density of oxide cathodes results from the very high local temperatures produced by ohmic heating of filaments and through Schottky barrier lowering. Cathode pulse behavior is explained by the breaking of filaments by thermal agitation and the subsequent regrowth of filaments. Dearnally's model contains many unknown parameters and would be difficult to quantify. The existence of sharply localized emitting regions is not consistent with spatially resolved work-function distributions obtained experimentally for oxide cathodes. The conducting filament concept does not appear to have gained much support.

#### 4. FAILURE MECHANISMS

There are a number of known failure mechanisms for oxide cathodes. Some mechanisms are intrinsic to conditions prevailing in a specific tube; they include the breakdown of the potting compound used on cathode heaters, damage by ion bombardment (to which ordinary oxide cathodes are quite susceptible),

poisoning by adsorbed electronegative species, and detachment of the oxide coating from the substrate. Any one of these mechanisms may be of practical importance, but they are outside the scope of the present discussion because they are tube specific. Some general failure mechanisms are discussed.

An attempt to draw excessive current from an oxide cathode will eventually result in a disruption of the oxide because of the effects of resistive heating. A resistance is associated with the oxide-ambient interface, and this resistance can increase, especially during pulse operation, as a result of donor depletion. In addition to the resistance of the surface region, and of the bulk, a resistance is encountered at the oxide-substrate interface. This resistance can increase with time as an insulating layer is formed through the reaction of the BaO with impurities, e.g., with silicon to form a barium orthosilicate. Excessive interfacial resistance can cause an internal spark discharge during pulse operation if high currents are drawn. The development of interfacial resistance can be controlled by proper initial purification of substrate material but can be a problem if quality control is not exercised. Poisoning of a cathode can of course result when bulk impurity species reach the surface. One recent study distinguishes between impurity effects on the Fermi level and on the electron affinity.<sup>24</sup> The formation of high-work-function patches of CaO slag of about 100 Å thickness has also been stated to result in failures of oxide cathodes.<sup>25</sup>

Barium is continuously evolved from an oxide cathode during operation. Evaporation rates of barium, strontium, and calcium from oxide cathodes have been measured by different methods including the use of radioactive tracers<sup>26</sup> and measurement of the effect of evaporated material on the thermionic emission of a tungsten probe wire.<sup>27</sup> The actual situation with regard to evaporation of material in a vacuum tube is complicated by the fact that material can re-evaporate and redeposit on the cathode from other parts of the tube. Barium loss ultimately should limit cathode life.

#### IV. BARIUM MONOLAYER CATHODES

A "monolayer" cathode consists of a metal base covered by an adsorbed electropositive species. More precisely, for practical cathodes, the adsorbed layer consists of an electropositive species coadsorbed with oxygen. A dipole layer is formed, and the work function of the adatom-substrate system can be lower than that of the initial substrate, and, in fact, lower than that of the bulk adsorbate. An examination of the periodic table indicates that cesium and barium monolayers should be particularly effective in lowering the surface work function since these elements are electropositive species of relatively large ionic radius. This expectation is confirmed experimentally.

Monolayer cathodes used in TWTs to date have all been based on barium. These cathodes are the dispenser and impregnated cathodes discussed later. Barium monolayer cathodes have higher work functions than alkaline earth oxide cathodes and therefore must be operated at a higher temperature for the same emission current density. However, higher emission current densities are possible than for oxide cathodes. Emission current densities on the order of several amperes per square centimeter can be obtained at operating temperatures of near 1100 C. These higher available current densities, combined with enhanced resistance to spark discharge and less sensitivity to air exposure during handling, make barium monolayer cathodes very attractive.

A surface monolayer of an alkali or alkaline earth on a substrate is volatile at the temperatures required for thermionic emission. Cesium is more volatile than barium, and, barium, therefore, is widely employed in practical cathodes. All barium monolayer cathode designs must provide for (1) the formation of a low-work-function surface monolayer and (2) the replenishment of evaporative loss from this monolayer during the operating life of the cathode.

## A. CONSTRUCTION

### 1. DISPENSER CATHODES

In a dispenser cathode, the two necessary conditions just described are satisfied by placing the barium compound that forms the work-function lowering layer in a cavity behind the base material, which is porous tungsten. The material in the cavity forms a reservoir to replenish the material lost from the cathode surface by evaporation.

The original dispenser cathode, the Phillips "L-cathode," is illustrated in Fig. 4.<sup>28</sup> A mixture of  $\text{BaCO}_3$  and  $\text{SrCO}_3$  is initially placed in the cavity. The porous tungsten plug has a density between 73 to 83% of the maximum theoretical density of tungsten. The carbonates are decomposed to oxides by heating in vacuo at about  $1100^\circ\text{C}$ . Barium reaches the surface during "activation," i. e., during further heating at a higher temperature. More details concerning these processes, and the different roles of barium and strontium, are given in Section IV. B.

An interesting variant of the dispenser cathode has been developed at the Naval Research Laboratory (NRL).<sup>29</sup> A regular mesh of iridium foil is used in place of the porous tungsten plug. Barium oxide is placed in a cavity behind the mesh. The chief advantage of this design is the possibility of very precise control of the barium arrival rate at the surface by the control of the mesh hole size and spacing. Further development work is in progress.

### 2. IMPREGNATED CATHODES

The "impregnated" cathode can be considered a type of dispenser cathode in which the alkaline earth mixture is not placed in a separate cavity but is distributed throughout the pores of the tungsten matrix (Fig. 5). In the original impregnated cathode (A-cathode), the impregnant starting mixture was  $5\text{BaCO}_3 \cdot 2\text{Al}_2\text{O}_3$ .<sup>30</sup> The A-cathode was superseded by the B-cathode, in which the starting impregnant is  $5\text{BaCO}_3 \cdot 2\text{Al}_2\text{O}_3 \cdot 3\text{CaCO}_3$ .<sup>31, 32</sup> The B-cathode can now be considered the "standard" impregnated cathode. A slight variation is found in the  $4\text{BaCO}_3 \cdot \text{Al}_2\text{O}_3 \cdot \text{CaCO}_3$  mixture of the Semicon S cathode.<sup>33</sup>

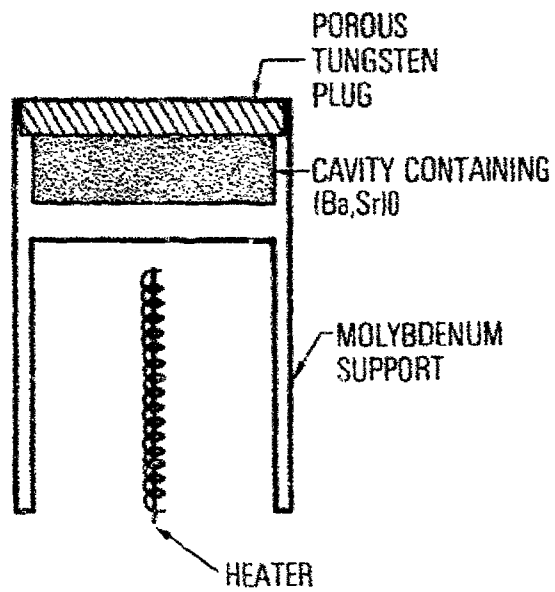


Fig. 4. L-Dispenser Cathode

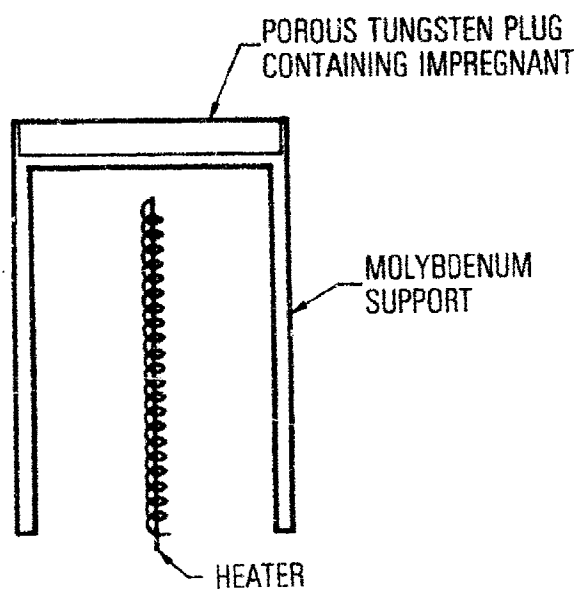


Fig. 5. Impregnated Cathode

Still other variants of the dispenser cathode are based on tungstate and scandate impregnants. In the tungstate cathode, a mixture of  $\text{BaCO}_3$ ,  $\text{SrCO}_3$ , and  $\text{WO}_3$  is heated to form a compound that can be represented by an expression such as  $\text{Ba}_5\text{Sr}(\text{WO}_6)_2$ . This mixture, in turn, is mixed with  $\text{ZrH}_2$  (an activator) and tungsten metal (90% by weight) to form a sintered cathode compact.<sup>34</sup> A similar procedure is employed to form scandate cathodes.

### 3. OSMIUM DISPENSER CATHODES

The Phillips M cathode has considerable promise for future Air Force applications.<sup>35</sup> The M cathode consists of a standard impregnated cathode on to which a thin (10,000 Å) surface layer of osmium has been deposited. The resultant surface has a work function lower than that of a conventional cathode. Phillips Corporation is no longer actively engaged in the manufacture of the M cathode. Some details of their manufacturing process have been given in a publicly available report commissioned by NASA;<sup>36</sup> however, certain steps in the procedures are described only in very qualitative terms.

#### B. PRINCIPLES OF OPERATION OF BARIUM MONOLAYER CATHODES

Some important questions that arise in connection with dispenser (including impregnated) cathodes are: (1) What is the nature of the low-work-function surface? (2) How are the activating species produced? (3) What is the mechanism by which these species reach the surface? and (4) What is the rate of evaporation of active species from the surface? The question as to what the mechanism is by which these species reach the surface involves both gaseous transport through the pores of the tungsten and diffusion along the tungsten surface. The (integrated) evaporation rate of the activating species, i. e., the impregnant, ultimately determines cathode life.

The structure of the low-work-function surface is considered in this section. The other questions posed will be addressed later for dispenser

and impregnated cathodes. An atom of an electropositive element, e. g., cesium or barium, adsorbed on a metal surface will ionize if the ionization potential of the adatom is less than the work function of the metal. In other words, ionization occurs if the energy gained by transferring an electron to the metal is greater than the energy required to remove the electron from the atom. The electron transferred to the metal enters the conduction band and is not localized. However, the adsorbed ionized species form a dipole layer in conjunction with their classical image charges. The dipole moment per unit area, i. e., the work-function change, is given by

$$\Delta\Phi = \frac{nqd}{\epsilon_0} \text{ (MKS units)} \quad (5)$$

where  $n$  is the number of adatoms per square centimeter,  $q$  is the ionic charge, and " $d$ " the dipole layer separation ( $d \approx 2r$ , where  $r$  is the ionic radius). The quantity calculated in Eq. (5) has the dimensions of an electrostatic potential (in volts), i. e., a change in energy per unit charge. The work function has been taken to be an energy in the previous discussion. However, since energy for electron emission is customarily measured in electron volts (the energy change when an electron moves through a potential difference of one volt), energy and electrostatic potential are related by a conversion factor of unit magnitude. The difference between potential and energy should be kept firmly in mind, however. Therefore, a capital  $\Phi$  is used in Eq. (5) for potential, whereas the work function as an energy is denoted by a lower case  $\phi$ .

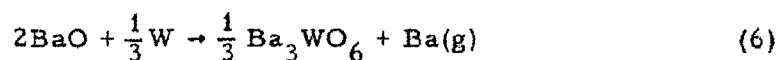
Complications in the application of Eq. (5) arise in practice. Adatoms interact, and the charge  $q$  is a function of surface coverage  $n$ . In addition, in practical cathodes, both an electropositive species and oxygen may be involved in the formation of the dipole layer. A more detailed discussion of these questions is given in Appendix B. The simple expression of Eq. (5) does, however, indicate that good thermionic emitters may be produced through the formation of appropriate surface monolayers on metallic substrates.

## 1. DISPENSER CATHODE

Schaeffer and White concluded that in the L-cathode the emitting surface is covered with barium, without a substantial amount of oxygen on the emitting surface or near the ends of the pores in the tungsten.<sup>37</sup> Barium coverage was said to be less than a complete monolayer. These authors suggested that a monolayer of residual oxygen initially present was removed from the tungsten by evaporating barium very early in the life of the cathode. The mechanism by which the oxygen removal is effected was not discussed. The evaporating material was identified as barium metal, not BaO (removal of a single surface monolayer of oxygen does not affect this conclusion).

Sharply differing conclusions and results were reached by Rittner et al. in a classic series of papers.<sup>38, 39</sup> Rittner et al. dealt with all four of the questions raised earlier. Measurements of surface diffusion, Knudsen flow, electron emission, and barium evaporation rate were carried out on tungsten of varying porosity. It was deduced that the L-cathode surface is covered by a complete monolayer of oxygen and that the oxygen, in turn, is covered by a complete monolayer of barium. The oxygen on the tungsten surface is responsible for both a lower work function than in the case of barium alone on tungsten and for a greatly increased sticking time for adsorbed barium.

Rittner et al. state that BaO is formed by thermal decomposition of the BaCO<sub>3</sub> with which the cathode is initially charged. The BaO then reacts with the tungsten in accordance with the following barium-producing reaction:



The gaseous barium is transported through the tungsten pores by Knudsen flow, and the barium picks up residual oxygen from the tungsten along the way. Rittner et al. found that half of the barium content in the evaporant is in the

form of BaO. The Knudsen flow of the barium through the pores is the rate-limiting step in barium evaporation (although it may not be the rate-determining step for barium coverage on the surface). Additional barium is formed through the reaction

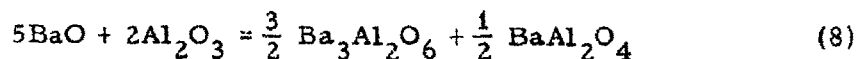


However, this reaction is postulated to be accompanied by the release of an oxygen-containing "poisoning agent" (not further specified) that results in the termination of cathode life.

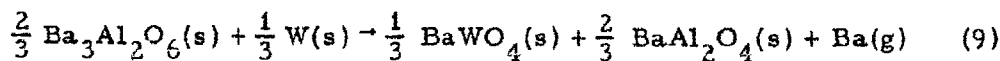
The emission of the  $\text{BaCO}_3 \cdot \text{SrCO}_3$ -filled cathode is quite similar to that of the  $\text{BaCO}_3$  cathode; however, the lifetime can be an order of magnitude greater. Rittner et al. attribute this lifetime increase to the fact that the equilibrium pressure of Ba + Sr vapor is lower than for the case of barium alone. The rate of barium release, which is far more than adequate to maintain monolayer barium coverage, is thus reduced, and cathode life is increased.

## 2. IMPREGNATED CATHODE

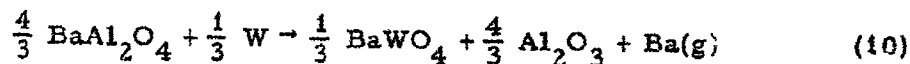
The impregnated cathode was also studied by Rittner and his coworkers, and, again, the questions of emitting surface composition, activation, and transport and evaporation of the active species were addressed.<sup>40</sup> The cathode investigated had the impregnant composition  $5\text{BaO} \cdot 2\text{Al}_2\text{O}_3$ ; it is known as the A-cathode (later formulations included CaO). The oxides in this ratio correspond to a eutectic mixture:



Barium is generated (on thermodynamic grounds) in accordance with the reaction



The  $\text{BaAl}_2\text{O}_4$  [Eq. (8) or (9)] can be considered inert with respect to the production of  $\text{Ba(g)}$  since the reaction



is, again on thermodynamic grounds, suppressed by the reaction of Eq. (9). Barium reaches the surface by Knudsen flow just as it does in the L-cathode. However, in contrast to the essentially constant evaporation rate of the L-cathode, the barium evaporation rate from the impregnated cathode was found to decrease as  $t^{-1/2}$ . The experimental data indicate that the evaporation rate is much higher than for the L-cathode during the first few hundred hours of life and is always sufficient to maintain a complete barium monolayer on the surface. Barium loss, of course, can occur both by evaporation from the surface monolayer or by direct streaming of material from the pores in the cathode matrix.

G. A. Haas and others at NRL carried out Auger analyses of impregnated cathodes and have made scanning low-energy electron probe (SLEEP) work function maps.<sup>41</sup> Auger electron spectroscopy provides an elemental analysis of the outer three to four atomic layers of a specimen surface; as a rough rule, elements present in concentrations as low as 1% of a surface monolayer are detectable. The SLEEP method provides work-function distribution information with 3- to 5- $\mu\text{m}$  spatial resolution and 30-mV energy resolution. In some cases, a correlation was observed between the presence of sulfur and early failure. On other cathodes with initially normal emission, more rapid than normal decay was found to correlate with a decrease in the barium, calcium, and oxygen peaks. This observed depletion is tentatively attributed to machining effects during fabrication that result in the blockage of pores in the tungsten. The cathode surface was found to be more similar to a BaO surface than to a barium surface. The BaO is one to several monolayers thick.

Springer and T. W. Haas of AFML measured chemical changes on dispenser cathodes during activation and poisoning by reactive gases by means

of Auger spectroscopy.<sup>42</sup> The concentration of surface species as a function of temperature was determined for a Type B Phillips cathode. It was concluded that in the normal cathode the ratio of barium to oxygen was 1, which is consistent with a tungsten surface covered by a monolayer of BaO.

Forman of NASA/Lewis has examined, by means of Auger spectroscopy, both actual cathodes and tungsten surfaces on which various species have been adsorbed.<sup>43,44</sup> His results differ in some respects from those of others and have generated some discussion. Forman compared Auger spectra from barium and BaO deposited on cleaned tungsten and oxidized tungsten with spectra of Phillips B and Semicon S cathodes. On the basis of the detailed structure of the low-energy Auger peaks of barium, he concluded that a monolayer of barium on a monolayer of oxygen is present on the (tungsten) surface of an impregnated cathode, as distinct from a layer of BaO on tungsten. These barium Auger peaks in the range 50 to 80 eV of kinetic energy differ in position, shape, and intensity for barium in the different chemical environments. Although Forman stressed this point, a careful examination of the papers by Rittner et al. and others does not indicate that distinguishing between Ba-O-W and BaO-W surfaces is really germane to the interpretation of the essential results of these other investigators. It is not clear whether describing a single layer of barium atoms on top of a single layer of oxygen atoms on a tungsten surface as an "oxide" or "not an oxide" is meaningful. The difference between "BaO on W" and "Ba on O on W" would basically have to do with the actual location of the surface dipole within a layer structure. As a scientific question, the issue merits further consideration, but its importance for practical cathodes is not clear.

The disagreement between Forman and Rittner on evaporation rate is more pertinent. On the basis of Auger measurements of barium desorption, Forman concluded that surface barium coverage must be less than one monolayer for much of the cathode life. This observation is the basis of a model

for cathode barium coverage and for the eventual end of cathode life. The extent of barium coverage represents an equilibrium between evaporative loss and the rate at which barium reaches the surface. Early in the life of the cathode, an adequate amount of barium is available, but as barium generated at the pore ends near the surface is depleted, surface coverage and electron emission decrease. Studies of "good" and "poor" cathodes have been described by Forman in which inadequate emission has been attributed either to poisoning or, in fact, to barium depletion.<sup>45</sup>

Forman's conclusions have been criticized.<sup>46</sup> Data on the B-cathode were recently made available that indicate that emission is nearly constant until the end of cathode life. Barium evaporation follows a  $t^{-1/2}$  law, just as for the A-cathode, and the total amount of barium given off, as calculated by integrating the evaporation data to the end of cathode life, corresponds to the amount of barium initially present. The calculated maximum lifetime for the particular cathode studied is  $10^5$  hr at  $1060^\circ\text{C}$  at the saturation emission current density of  $5\text{ A/cm}^2$ . The observed constant emission implies that cathode barium coverage does not change with time, and, in fact, the available data indicate that a full barium monolayer is always present until the end of cathode life. As an explanation of the discrepancies between Forman's results and the observations for B-cathodes, it was suggested that the deposited barium films used by Forman to determine evaporation rate are not representative of impregnated cathodes. Although the work function of a barium on oxygen on tungsten surface is not critically dependent on oxygen content (in agreement with Forman), barium evaporation does depend strongly on oxygen content. Forman's surfaces are described as oxygen deficient. On an actual cathode, surface oxygen is presumed to be replenished from the BaO streaming from the interior.

It is apparent that in spite of the considerable effort put forth by several research groups over the past decades our understanding of impregnated cathodes is incomplete.

### 3. OSMIUM DISPENSER CATHODES

In a search for a lower work-function surface monolayer-substrate system, it is possible to vary both the adsorbate and the substrate material. It perhaps seems paradoxical, but an increase in substrate work function results in a decrease in the minimum work function attainable for a given adsorbate. This interesting result is explained by a qualitative argument.<sup>47</sup> The electrostatic potential energy near a metal surface is shown without and with a surface monolayer of a readily ionizable cation species in Figs. 6a and 6b, respectively. The work function lowering is given by Eq. (5), and is proportional to the product of the number density of cations and their charge, as in "ordinary" monolayer cathodes (Section IV. B). The available electron of the adatom lies at the bottom of a potential well of depth  $I_{ads}$ .  $I_{ads}$  is measured with respect to the local electrostatic potential, which may differ from the vacuum or zero level (Fig. 6).

As the number of adatoms increases, the local potential energy  $\phi(x)$  ( $x$  is the spatial coordinate perpendicular to the surface) is depressed, but the ionizable adatom level remains at  $I_{ads}$  below the local potential  $\phi(x = r)$  ( $r$  is the cation radius).  $\phi(r)$  can be depressed only until  $I_{ads}$  coincides with the Fermi level, at which point the greatest work function lowering is achieved. If the adatom density increases further, the average adatom charge must decrease. The electrostatic potential energy is constrained to be at  $I_{ads}$  above the Fermi level at  $x = r$  and to be  $\phi_0$  above the Fermi level just at the metal surface. In Fig. 6d, it is evident that these constraints mean that an increase in substrate work function  $\phi_0$  actually lowers the work function of the monolayer system (provided  $I_{ads} < \phi_0$ ).

This qualitative explanation of the osmium dispenser cathode may be placed on a more quantitative basis by a classical electrostatic argument.<sup>47</sup> A uniform layer of adsorbed cations on a metal with  $N$  cations/cm<sup>2</sup> is considered. The equivalent area per cation is  $\pi R^2 = 1/N$ , and  $r$  again denotes the cation radius. The local potential at an ion can be calculated if it is assumed

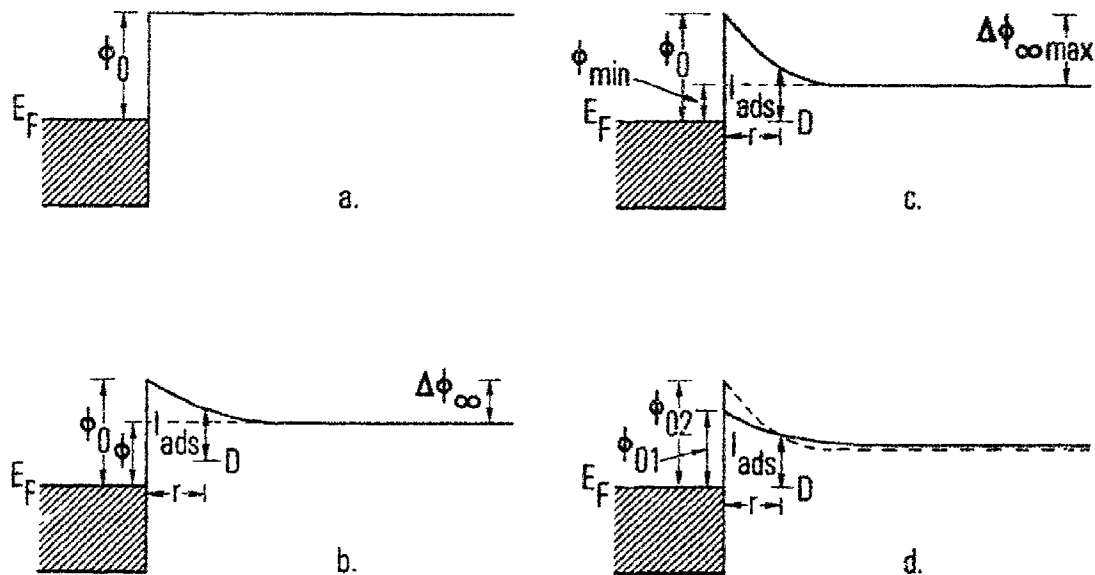


Fig. 6. Potential Energy Diagrams Illustrating Additional Work-Function Lowering Obtained with Monolayer Cathode as Result of Increasing Substrate Work Function. a. With no adsorbed donor species, potential energy distribution is just that for (assumed ideal) metal substrate. Work function  $\phi_0$  is (by definition) energy interval between Fermi level and vacuum level. b. When some adsorbed donor species are present, dipole layer is formed and work function is reduced from  $\phi_0$  to  $\phi$ . Adatoms appear as localized levels  $D$  at an energy interval  $l_{ads}$  below local potential and at distance  $r$  from the surface. c. At optimum adatom coverage, donor levels  $D$  coincide with Fermi level of substrate. Work function has minimum value  $\phi_{min}$ . d. Potential energy curve is constrained to lie at  $\phi_0$  above Fermi level just at substrate surface and to value  $l_{ads}$  above Fermi level at adatom distance  $r$  for minimum work function of adsorbent-adsorbate system. A higher substrate work function ( $\phi_{02}$ , dashed curve) results in lower minimum work function for the system than does a lower substrate work function ( $\phi_{01}$ , solid curve). Adatom concentration for optimum coverage may differ for different substrate work functions.

that one ion is removed from the surface, leaving a circular hole of radius  $R$ . The corresponding distribution of charges is represented by a uniform positive charge layer at distance  $r$  above the surface and a negative image charge layer a distance  $r$  behind the surface, and by a negative disk (of the same charge density as the original layer) at  $r$  above the surface and a positive image charge disk at  $r$  behind the surface. The potential along the line of symmetry between two parallel coaxial oppositely charged disks is easily calculated. With the potential of the disks and of the uniform charge layers superimposed, the potential energy difference between the center of an ion and the metal surface is

$$\Delta\phi = \sqrt{\pi N} (\sqrt{1 + 4\pi r^2 N} - 1) \frac{e^2}{2\pi \epsilon_0} \quad (11)$$

where  $e$  is the electronic charge. When  $N = N_{\text{opt}}$ , the optimum coverage for work-function lowering,  $\Delta\phi = \phi_0 - I_{\text{ads}}$ . Furthermore, there is the relation

$$\phi_0 - \phi_{\text{min}} = N_{\text{opt}} \frac{re^2}{\epsilon_0} \quad (12)$$

An explicit expression thus can be obtained for  $\phi_{\text{min}}$  in terms of  $\phi_0$  and  $I_{\text{ads}}$ , and it is easily verified that  $d\phi_{\text{min}}/d\phi_0 < 0$ , as asserted previously.

The investigation of different metal coatings of higher work function than tungsten that do not react with the impregnant resulted in the development of the Phillips M-cathode. Rhenium, ruthenium, iridium, and osmium all meet the essential requirements. An osmium plus 20% ruthenium coating 5000 to 15000-Å thick is sputter-deposited on the surface of an ordinary dispenser cathode to produce the M-cathode. Osmium loss apparently does not occur during the life of an M-cathode.<sup>48</sup> Emission current density decreases

as the result of the formation of an  $\text{OsW}_2$  alloy, which has a work function essentially equal to that of a pure tungsten surface and, after thousands hours of operation, the M-cathode becomes similar to the standard B-cathode without an osmium coating.

Analyses of M-cathode surfaces have recently been reported.<sup>49</sup> A "columnar" structure was observed in scanning electron micrographs of the sputter overcoat. The columns are 1/2 to 1  $\mu\text{m}$  across and may play a role in the cathode function by increasing the effective surface area. X-ray photoelectron spectroscopy data on an activated M-cathode indicated that the tungsten was metallic, not oxidized.<sup>49</sup>

#### 4. FAILURE MECHANISMS

Although a monolayer cathode ultimately must fail by depletion of the active material, other failure modes, in practice, occur first. These failure modes are under active investigation in several laboratories. Cracking and dimensional changes have been observed. Porous tungsten is also not stable with respect to a loss of pore volume by sintering.

page 38 blank

## V. OTHER MONOLAYER CATHODES

Monolayer cathodes, other than the barium dispenser and impregnated types, have no history of use in spacecraft TWTs. A discussion of "other" monolayer cathodes is included here both for completeness and because some consideration has been given to the use of  $\text{LaB}_6$  in TWTs.

### A. THORIATED TUNGSTEN CATHODES

Thoriated tungsten cathodes have long been used in radio frequency transmitting tubes. They provide rather high current densities and have long operating life; however, their operating temperatures and work function are significantly higher than those of cathodes based on barium.

Thoriated tungsten cathodes are produced by adding 1 to 2% thorium oxide to tungsten powder, then sintering, swaging, and drawing the material to form wire filaments. The filament is heated to  $\approx 2500^\circ\text{C}$  for several minutes, then held at  $1825^\circ\text{C}$  for 30 min. The normal operating temperature is  $\approx 1625^\circ\text{C}$ . Improved performance is achieved if the filament is heated in a hydrocarbon atmosphere to form a tungsten carbide surface layer. The thermal efficiency is higher, and the operating temperature of the thoriated tungsten filament is lower than for pure tungsten; however, thoriated tungsten filaments are more susceptible to damage by bombardment by residual gas ions.

Thorium monolayer cathodes analogous to barium dispenser cathodes have been constructed also. One such cathode is made with a tungsten, thorium, and tungsten carbide mixture in a tungsten or tungsten rhenium cup.<sup>50,51</sup> In another design, a thorium carbide-tungsten eutectic is drawn by capillary action into a tungsten dendrite matrix.<sup>52</sup> This cathode is said to be more resistant to hydrolysis and to be mechanically stronger than the packed powder design. These cathodes were developed by General Electric.

It has long been thought that a surface monolayer of thorium is responsible for the emissive properties of thoriated tungsten.<sup>53</sup> Thorium,

an electropositive species, could form a surface monolayer that would result in a surface of reasonably low work function ( $\sim 2.6$  eV for the thoriated tungsten cathode). Recent measurements by means of Auger electron spectroscopy confirm that the surface of thoriated tungsten is enriched in thorium ( $\text{Th/O} \approx 40$  for an activated cathode).<sup>54</sup> Carbonized thoriated tungsten is apparently covered also by a thorium monolayer.

#### B. LANTHANUM HEXABORIDE CATHODES

Lanthanum hexaboride cathodes are now widely used in scanning electron microscopes and other laboratory instruments where a small, bright electron source is desirable. The  $\text{LaB}_6$  cathode is in the form of a pointed, indirectly heated rod for such applications, although for other uses other configurations could presumably be employed. The  $\text{LaB}_6$  cathodes have good tolerance to exposure to air (when cool), which recommends their use in laboratory instrumentation. The work function and operating temperature of  $\text{LaB}_6$  cathodes are higher than barium-based cathodes, but the robust nature of  $\text{LaB}_6$  cathodes does suggest their possible use in TWTs.

One might question the classification of  $\text{LaB}_6$  cathodes as monolayer cathodes. It was originally proposed that the  $\text{LaB}_6$  cathode was enriched by lanthanum that diffused to the surface to form a dipole layer.<sup>55</sup> The latest Auger evidence and mass spectrometric analysis of evaporant materials are in contradiction with this hypothesis.<sup>56</sup> The low work function of  $\text{LaB}_6$  is apparently intrinsic to the material. However, it is likely that the outermost atomic layer of  $\text{LaB}_6$  is indeed a lanthanum plane, and a surface dipole does exist as it must at the surface of any material.  $\text{LaB}_6$  happens to have a dipole of proper sign (on the appropriate crystal faces) and a sufficiently high melting temperature to make it a useful thermionic emitter. Other rare earth hexaborides have also been investigated, mostly by Soviet researchers.

## VI. TEST PROCEDURES AND LIFE-TEST DATA FOR THERMIONIC CATHODES

Requirements of different agencies concerned with TWTs for satellite use may vary. Space Division has a requirement for a cathode capable of delivering 1 to 2 A/cm<sup>2</sup> for 7 to 10 years (~60,000 to 90,000 hr).

It is not possible to assess cathode performance without some criteria for cathode failure and the end of cathode life. The end of cathode life in TWT applications does not necessarily imply total cessation of emission. The area of the cathode emitting surface is as much as 50 times larger than the final area of the electron beam. The cathode surface is concave, and electrons are focused before entering the traveling-wave structure. Even a slight degradation of cathode emission can change the space-charge distribution sufficiently to defocus the electron beam. The power in the beam is more than sufficient to destroy the traveling-wave structure if the beam wanders. A general discussion of TWTs is presented in Ref. 7.

Various empirical methods for assessing cathode condition are used. One standard method involves shutting off cathode heater power, then recording the time required for emission to drop to some fraction of its initial value. This "time-to-knee" method is valid only for comparing cathodes of identical type and construction. In other life tests, cathode failure is defined as the point at which cathode temperature must be increased above some arbitrary value to maintain a given current density. Still other criteria are, of course, possible.

The selection of the "test vehicle" is another unresolved problem in assessing cathode performance. Many tests have been carried out with cathodes in a simple diode configuration. Unfortunately, the cathode interacts with the remainder of the tube. For example, evaporated material may be transferred from the cathode to an intermediate surface and back to the

cathode. In some test configurations, TWT geometry is simulated, and more widespread use of such configurations has been advocated. It must then be decided whether appropriate bias and radio frequency voltages should also be present. Inclusion of these additional factors greatly increases the complexity and cost of cathode life tests. Considerable discussion at the recent Tri-Service Cathode Workshop was devoted to this question of test standardization.

The lack of standardized test procedures complicates comparisons of cathode life-test data. A further complication is the simple fact that the very-long-term life-test data essential for space tube cathodes are just not available. Life tests, especially those in which actual tubes or simulated tube geometry are used, are expensive, and accelerated tests are suspect because of the many variables involved. Extrapolation of observed degradation to forecast ultimate tube life is not necessarily straightforward.

Space experience with oxide cathodes in commercial satellites is summarized in Ref. 7. For 100,000 hr, it is suggested that cathode current density should not exceed  $0.2 \text{ A/cm}^2$ .

Some long-term test data for dispenser cathodes are available. Information given in Ref. 7 indicates that a lifetime in excess of  $10^5$  hr at  $1035^\circ\text{C}$  for an S-type impregnated cathode is possible. This estimate is based on an extrapolation of higher temperature data, and the current density is not specified. There is some evidence from European manufacturers, including both test data and flight experience, that dispenser cathodes may meet Air Force requirements. More information, however, is needed.

Long-term life tests are now in progress at Hughes Electron Dynamics Division and at Watkins-Johnson, Inc. The Watkins-Johnson data are of particular interest since the B, M, S, and tungstate cathodes were all evaluated in a simulated tube geometry at  $2 \text{ A/cm}^2$ .<sup>57</sup> The tungstate cathode was found to be unsatisfactory in the Watkins-Johnson test, although other published data are somewhat more encouraging.<sup>58</sup> In contrast to the results

of Ref. 7, the S-cathode also did not perform very well. The impregnated cathodes, the B-cathode, and especially the M-cathode, seem to be more promising for Air Force missions.

*page 44 blank*

## VII. FIELD-EMISSION CATHODES

Processes other than thermionic emission, e. g., photoemission and secondary emission, can be employed to provide an electron source. Of all possible nonthermionic cathodes, however, field emitters seem to be the most appropriate for space applications.

Application of an electric field lowers the energy barrier for electron emission (Schottky effect, Appendix A). Stanford Research Institute has recently described a technique in which microcircuit fabrication methods were used for producing an array of cones on a surface (Fig. 7).<sup>59</sup> About  $6.4 \times 10^5$  cones/cm<sup>2</sup> can conveniently be produced. At an applied potential of 50 to 200 V on the molybdenum overcoat, each cone emits  $\sim 150 \mu\text{A}$ , for a total emission of  $\sim 95 \text{ A/cm}^2$ . Another field emitter cathode technology has been described in which an array of tungsten fibers is produced in a UO<sub>2</sub> rod.<sup>60</sup> The fiber density is  $1 \times 10^7$  to  $5 \times 10^7$ /cm<sup>2</sup>, and the sharp fiber ends serve as field emission points on the surface. NRL has incorporated an SRI-cathode in an actual tube (purely for demonstration purposes).

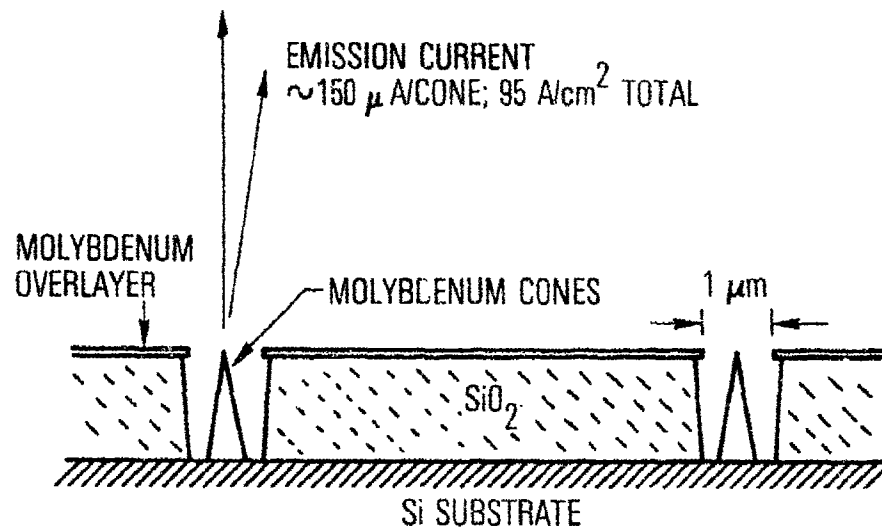


Fig. 7. Stanford Research Institute Field-Emission Cathode

## VIII. CONCLUSIONS

Many different types of thermionic cathodes, as well as some types of field emitter cathodes, have been described in this report. Studies of thermionic emission from still other types of cathodes, including various carbides, borides, rare earth oxides, and other rather exotic materials can be found in the literature. However, cathode research in the United States has not been funded extensively in recent decades. A number of agencies have developed or adopted a "favorite" cathode and have undertaken limited development work, but systematic studies of thermionic emission by means of modern surface-analysis techniques have generally been lacking. With the notable exception of work undertaken at NRL, cathode studies in recent years usually have been initiated only in response to specific problems.

The results of a literature survey undertaken during the preparation of this report may be of general interest. A computerized search (Lockheed Dialog system) of the Inspec (IEE of the U. K.) data base was made with the search terms thermionic cathode(s) or thermionic emission or oxide cathodes. A total of 566 references was found for the period January 1969 to May 1978. Several hundred references, from the mid-1970s to the present, were sorted by country of origin. Nearly half of the papers originated in the Soviet Union and Eastern Europe. About 20% of the publications were from the United States, 17% from Western Europe, and 10% from Japan. The studies of "exotic" thermionic emitters have almost all been carried out in the Soviet Union.

Informed sources within the cathode community indicate that dispenser-impregnated cathodes will have to be employed to meet future spacecraft mission requirements. Of these cathodes, the impregnated B-cathode and osmium coated M-cathode offer the highest probability of success. There are no fundamental reasons why more exotic emitters, e. g., field emitters, could

not ultimately be employed in space applications. However, the difficulty in acquiring sufficient test data in any reasonable time to flight-qualify components based on a new technology, even with no gross problems in fabrication and operation, is so great that impregnated cathodes will almost certainly be utilized. Test data on impregnated cathodes are still not complete, but encouraging data do exist.

Although impregnated cathodes are promising, there are many unresolved questions. Cathode performance varies. Reproducibility in impregnated-cathode fabrication is essential if they are to be used with confidence in space tubes. Reproducibility must ultimately depend on a thorough understanding of impregnated-cathode operation, e. g., on the importance of surface morphology and impurities. During the next few years, additional studies of impregnated-cathode surfaces by means of modern surface analytical techniques must be undertaken. Such studies should correlate information obtained through submicron Auger analysis and work-function mapping. Detailed analyses of this type should permit the identification of specific cathode failure mechanisms, the correlation of cathode performance with these failure processes, and the development of means of recognizing signatures indicative of premature cathode failure. Having thus elucidated the basic failure mechanisms of TWT cathodes, the objective of improved cathode performance would be met by means of (1) recommendations on material and process improvements, (2) improved methods for cathode quality control, and (3) guidelines for accelerated testing and lifetime prediction.

Additional studies of other types of thermionic cathodes, and of non-thermionic emitters as well, should also be funded. It should be possible, by means of modern analysis techniques, to effect a considerable advance in the understanding of the electron emission process. Research on cathode technology is likely to be very cost effective in view of the enormous cost of the communications satellites that are absolutely dependent upon it.

## REFERENCES

1. Defense Satellite Communications Office, TOR-0074(4624-01)-2 The Aerospace Corporation (1 February 1974).
2. C. Herring, and M. H. Nichols, Rev. Mod. Phys. 21, 185 (1949).
3. W. B. Nottingham, Thermionic Emission, Report 321, MIT Research Laboratory of Electronics Technology, Cambridge, Mass. (10 December 1956).
4. A. Venema, "Thermionic Emission," in Handbook of Vacuum Physics, Vol. II, Chapt. 2, A. H. Beck, ed., Pergammon Press, Oxford (1966).
5. R. O. Jenkins, Vacuum 19, 353 (1969).
6. R. Strauss, J. Bretting, and R. Metivier, Proc. IEEE 69, 387 (1977).
7. G. A. Haas and R. E. Thomas, "Thermionic Emission and Work Function," in Techniques of Metals Research, Vol. 6, Part 1, E. Passaglia, ed., Interscience, New York (1972).
8. J. M. Housten, and H. F. Webster, "Thermionic Energy Conversion," in Advances in Electronics and Electron Physics, Vol. 17, L. Martin, ed., Academic Press, New York (1962).
9. G. A. Haas and R. E. Thomas, J. Appl. Phys. 34, 3457 (1963).
10. G. A. Haas and R. E. Thomas, Surf. Sci. 4, 64 (1966).
11. J. D. Ryder, Electronic Fundamentals and Applications, Prentice-Hall, Englewood Cliffs, New Jersey (1959).
12. C. P. Hadley, W. G. Rudy, and A. G. Stoeckert, J. Electrochem. Soc. 105, 395 (1958).
13. G. Medicus, 1978 Tri-Service Cathode Workshop, Naval Research Laboratory, Washington, D.C., 1978.
14. D. W. Mauer and C. M. Pleass, Bell System Tech. J. 2375 (1967).
15. L. S. Nergaard, RCA Rev. 20, 191 (1959).

16. K. M. Tischer, Vakuum Tech. 15, 114 (1966).
17. L. S. Nergaard, RCA Rev. 13, 464 (1952).
18. R. H. Plumlee, RCA Rev. 17, 231 (1956).
19. T. N. Chin, R. W. Cohen, and M. D. Coutts, RCA Rev. 35, 521 (1974).
20. R. Loosjes and H. J. Vink, Phillips Res. Reports 4, 449 (1949).
21. R. C. Hughes and F. P. Coppola, Phys. Rev. 88, 364 (1952).
22. N. A. Surplice, Brit. J. Appl. Phys. (J. Phys. D) 1, 1245 (1968).
23. G. Dearnalley, Thin Solid Films 3, 161 (1969).
24. G. A. Haas, A. Shih, and R. E. Thomas, 1978 Tri-Service Cathode Workshop, Naval Research Laboratory, Washington, D.C., 1978.
25. A. Shih, G. A. Haas, and C. Hor, 1978 Tri-Service Cathode Workshop, Naval Research Laboratory, Washington, D.C., 1978.
26. W. F. Leverton and W. G. Shepherd, J. Appl. Phys. 23, 787 (1952).
27. W. C. Rutledge, A. Milch, and E. S. Rittner, J. Appl. Phys. 29, 834 (1958).
28. H. J. Lemmens, M. J. Jansen, and R. Loosjes, Phillips Tech. Rev. 11, 341 (1950).
29. R. E. Thomas, T. Pankey, and G. A. Haas, 1978 Tri-Service Cathode Workshop, Naval Research Laboratory, Washington, D.C., 1978.
30. R. Levi, Appl. Phys. 24, 233 (1953).
31. R. Levi, Appl. Phys. 26, 639 (1955).
32. R. Levi, Phillips Tech. Rev. 19, 186 (1957/58).
33. Semicon Dispenser Cathodes, Semicon Associates, Inc., Lexington, Kentucky, undated technical bulletin.
34. R. J. Bondley, W. T. Boyd, T. J. Mall, and M. J. Silvka, ECOM-01719-15-3, Research and Development Technology, Schenectady, New York (1969).

35. P. Zalm and A. J. A. van Stratum, Phillips Tech. Rev. 27, 69 (1966).
36. A. Gupta and C. O. Young, The Manufacture of M-Type Impregnated Cathodes, for Order No. C-2129-D, NASA/Lewis Research Center (1977).
37. D. L. Schaeffer and J. E. White, J. Appl. Phys. 23, 669 (1952).
38. E. S. Rittner, R. H. Ahlert, and W. C. Rutledge, J. Appl. Phys. 28, 156 (1957).
39. W. C. Rutledge and E. S. Rittner, J. Appl. Phys. 28, 167 (1957).
40. E. S. Rittner, W. C. Rutledge, and R. H. Ahlert, J. Appl. Phys. 28, 1468 (1957).
41. G. A. Haas, H. F. Gray, and R. E. Thomas, J. Appl. Phys. 46, 3293 (1975).
42. R. W. Springer and T. W. Haas, J. Appl. Phys. 45, 5260 (1974).
43. R. Forman, TN O-8295, NASA-Lewis (1976).
44. R. Forman, J. Appl. Phys. 47, 5272 (1976).
45. R. Forman, IEEE Trans. Electron. Devices ED24, 56 (1977).
46. E. S. Rittner, J. Appl. Phys. 48, 4344 (1977).
47. P. Zalm and A. J. A. van Stratum, Phillips Tech. Rev. 27, 69 (1966).
48. A. J. A. Van Stratum and P. N. Kuin, J. Appl. Phys. 42, 4436 (1971).
49. D. Jones, 1978 Tri-Service Cathode Workshop, Washington, D. C. 1978.
50. H. H. Glascock, Jr., J. Appl. Phys. 37, 4995 (1956).
51. H. H. Glascock, Jr., Rev. Sci. Inst. 43, 698 (1972).
52. H. H. Glascock, Jr., Rev. Sci. Inst. 47, 90 (1976).

53. W. E. Danforth, "Thorium Oxide and Electronics," in Advances in Electronics and Electron Physics, Vol. V, L. Marton, ed., Academic Press, New York (1953).
54. K. Ishikawa and H. Tobase, Japan J. Appl. Phys. 15, 1571 (1976).
55. J. M. Lafferty, J. Appl. Phys. 22, 299 (1951).
56. B. Goldstein and B. J. Szostak, J. Appl. Phys. (to be published).
57. D. H. Smith, R. R. Bartsch, and G. Woda, CR-134602, NASA (1974).
58. B. Smith and A. Newman, IEEE Trans. Electron. Devices ED24, 279 (1977).
59. J. Brodie and C. A. Spindt, 1978 Tri-Service Cathode Workshop, Naval Research Laboratory, Washington, D. C., 1978.
60. W. L. Ohlinger, D. N. Hill, R. K. Feeny, and A. T. Chapman, 1978 Tri-Service Cathode Workshop, Naval Research Laboratory, Washington, D. C., 1978.

## APPENDIX A

### EMISSION EQUATIONS

#### A. THERMIONIC EMISSION FROM METALS

Thermionic emission from metals provides a convenient starting point for a general discussion of thermionic emission. Certain concepts fundamental to an understanding of thermionic emission, e. g., work function, are easier to visualize for a metallic emitter.

The thermal emission of electrons from a metal is analogous to the evaporation of molecules from a liquid. In both cases, particles with sufficient kinetic energy can overcome an energy barrier and escape. The electrons in a metal constitute a degenerate gas and must be described by means of Fermi statistics. At absolute zero temperature, each possible energy level is occupied by two electrons to a maximum value known as the Fermi energy (Fig. A-1). This energy boundary between occupied and unoccupied energy levels is sharply defined at 0 K. At a temperature  $T > 0$ , the boundary region is roughly of width  $kT$  (where  $k$  is the Boltzmann constant). Only electrons in this interval,  $kT$ , are capable of absorbing small (thermal) amounts of energy. The Pauli exclusion principle forbids thermal excitation of electrons farther down in the energy distribution since no unoccupied state is available to receive them. The Fermi energy is defined at temperature  $T$  as the energy of that level with a probability of occupation of 0.5. The minimum energy that an electron must have to escape from the metal (at absolute zero) is the energy difference between the Fermi level and the vacuum level; this quantity is the work function. The work function is a characteristic of the bulk metal and depends upon the surface state of the metal, including crystal orientation. For the moment, it is simply assumed that the work function is constant everywhere on the ideal metal surfaces considered in the next several sections.

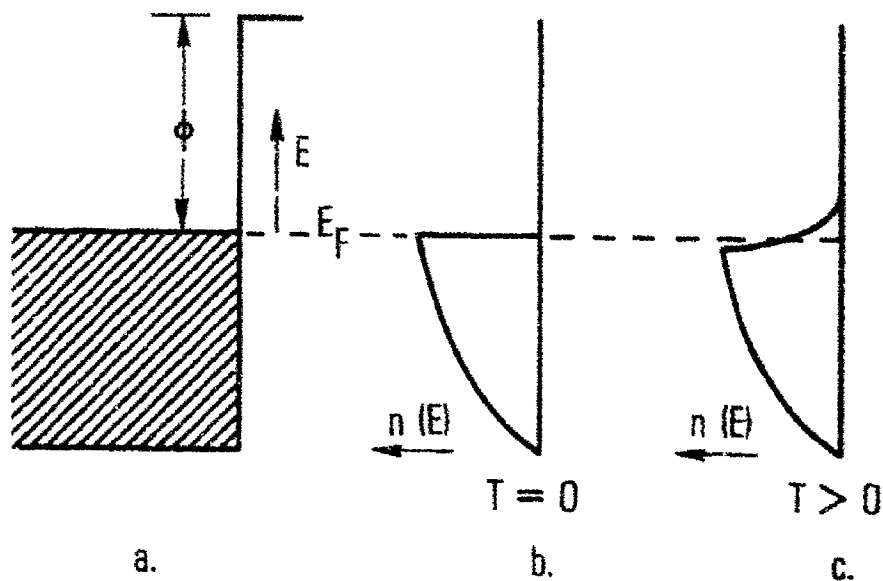


Fig. A-1. a. Energy-Level Diagram for Metal and Corresponding Density of Electron States. b. At  $T = 0$  K. c. At  $T > 0$  K.  $E_F$  is the Fermi level;  $\phi$  is the work function.

## 1. RICHARDSON-DUSHMAN EQUATION

Certain equations involving electron emission current arise repeatedly in any discussion of cathodes. The emission current from a metal at temperature  $T$  is readily calculated. A standard derivation is presented first.<sup>1</sup>

The momentum distribution for the electrons in a Fermi gas, i. e., the number of electrons per unit volume with momentum between  $\vec{p}$  and  $\vec{p} + \Delta\vec{p}$ , is

$$n(\vec{p}) = \frac{2}{h^3} \frac{1}{1 + \exp[(E - E_F)/kT]} \quad (\text{A-1})$$

where  $E_F$  is the Fermi energy with respect to the vacuum level, and  $E$  is the electron energy measured with respect to the Fermi level. The  $x$  axis is assumed to be normal to the surface; the emitted electron current will simply be  $(-e)$  times the rate at which electrons cross the surface in the  $x$  direction. Since the rate at which electrons in the momentum range  $d\vec{p}$  strike the surface is

$$v_x n(\vec{p}) d\vec{p} = \frac{\partial E}{\partial p_x} n(\vec{p}) d\vec{p} = n(\vec{p}) dE dp_y dp_z$$

the emitted current is

$$J = \frac{2e}{h^3} \int_{-\infty}^{\infty} \int_{-\infty}^{\infty} \int_{\phi + E_F}^{\infty} dp_y dp_z dE \frac{1}{1 + \exp[(E - E_F)/kT]} \quad (\text{A-2})$$

The zero of energy in Eq. (A-2) is taken as the bottom of the conduction band (Fig. A-1). Since  $(E - E_F)/kT \gg 1$  the above integral can be approximated by

$$J = \frac{4\pi m e}{h^3} (kT)^2 e^{-\phi/kT} \quad (\text{A-3a})$$

Equation (A-3) is prominent in any discussion of cathodes and is known as the Richardson-Dushman equation. The equation is often written in the form

$$J = AT^2 e^{-\phi/kT} \quad (\text{A-3b})$$

where

$$A = \frac{4\pi m e k^2}{h^3} = 120 \text{ A}/(\text{cm}^2 \text{ K}^2)$$

is the universal thermionic (Richardson) constant. As originally derived by Richardson, the temperature dependence in the pre-exponential is  $T^{1/2}$ , not  $T^2$ . Soon after the development of quantum mechanics, Dushman correctly derived the  $T^2$  dependence (although Dushman missed by a factor of two because the electron spin still had not been discovered at the time of his derivation). Experimental values of the Richardson constant can depart widely from the theoretical value  $120 \text{ A}/\text{cm}^2 \text{ K}^2$ . An interesting correlation between measured values of the Richardson coefficient and the heats of atomization of the emitting surfaces has been noted.<sup>2</sup> However, this correlation evidently arises, at least in part, because of the effect of the material evaporated from the cathode on the anode work function and therefore is not intrinsic to the emission process.

It has been assumed that electrons reaching the surface with sufficient energy and with appropriately directed velocity inevitably are emitted. There is a possibility that electrons may be reflected back into the metal. Therefore, the Richardson-Dushman equation often is written in the form

$$J = A(1 - \bar{r}) T_e^2 e^{-\phi/kT} \quad (\text{A-3c})$$

where  $\bar{r}$  is a reflection coefficient, which can, at least in principle, be calculated.

Equation (A-3) was derived with the assumption of a particular energy distribution in the metal. The equation can also be derived in a very general way by means of statistical mechanics.<sup>3</sup> The emitter is taken to be in equilibrium with the gas of emitted electrons outside the metal. This derivation makes clear the interesting fact that measurements of emitted current never yield information about the microscopic structure of the emitter except to the extent that this structure influences the work function or the reflection coefficient. Band structure effects on the reflection coefficient, which are generally negligible, are treated in Ref. 4.

## 2. LANGMUIR-CHILD EQUATION

A diode vacuum tube consisting of an ideal cathode and an anode is considered. If a positive anode voltage  $V_A$  is increased from zero, a limiting current described by the Richardson-Dushman equation (Eq. A-3) is reached. This situation is known as temperature-limited emission. At lower anode voltages, emission current may be sufficient to produce a space-charge region between the anode and cathode.<sup>5,6</sup> The voltage between the anode and the cathode must obey Poisson's equation:

$$\frac{d^2 V}{dx^2} = \frac{-\rho(x)}{\epsilon_0} \quad (\text{A-4})$$

where  $\rho(x)$  is the charge density. The equation of continuity requires that  $J(x) = \text{constant} = J$ . If electrons are emitted from the cathode with zero velocity,

$$\left(\frac{1}{Z}\right) mv^2 = eV(x) \quad (\text{A-5})$$

Furthermore, since  $J = \rho v$ , Eq. (A-4) can be written

$$\frac{d^2V}{dx^2} = \frac{1}{\epsilon_0} \left(\frac{m}{Ze}\right)^{1/2} \frac{J}{V^{1/2}} \quad (\text{A-6})$$

One may solve for  $V(x)$ . Utilization of the boundary condition that at  $x = L$ ,  $V(x) = V$ , the applied voltage, results in the expression

$$J = \frac{4\epsilon_0}{9} \sqrt{\frac{Ze}{m}} \frac{1}{L^2} V^{3/2} \quad (\text{A-7})$$

relating the current and the applied voltage for a simple diode configuration. This expression is known as the Langmuir-Child law. Electrons are in fact not emitted with zero kinetic energy as assumed in the above derivation. A more complete solution to the diode current problem, including the effect of the finite initial velocity of the electrons, is given in Ref. 5.

### 3. SCHOTTKY BARRIER LOWERING

The applied field itself can influence the emission current by effectively lowering the cathode work function.<sup>6</sup> An electron outside a metal (taken to be a semi-infinite conducting sheet) "sees" an image charge and experiences a potential (Fig. A-2):

$$\Phi(x) = \frac{e}{16\pi\epsilon_0 x} + \text{constant} \quad (\text{A-8})$$

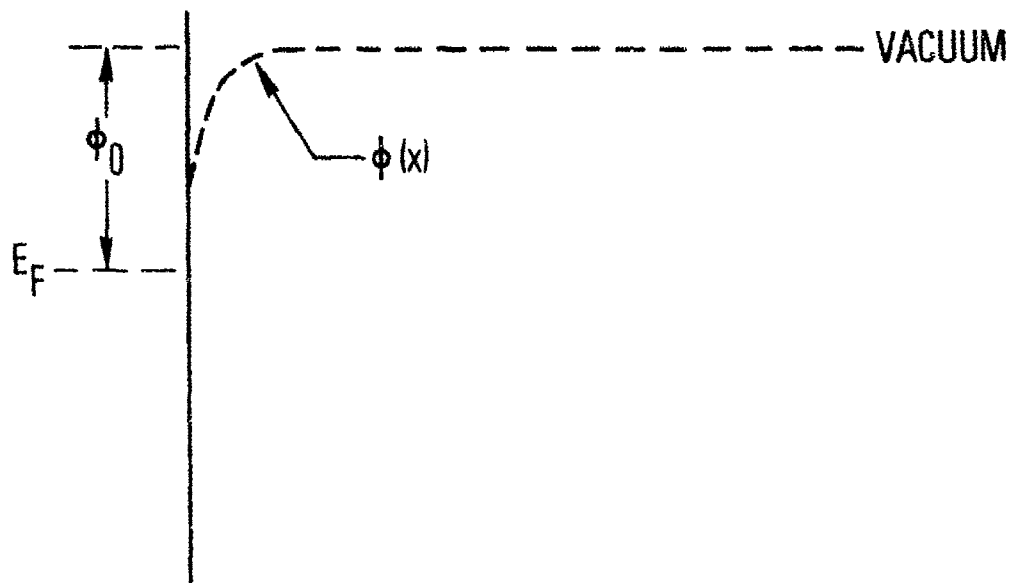


Fig. A-2. Electron Energy as Function of Distance from Surface of Metal in Absence of Applied Field

As the electron approaches the surface, it will eventually "see" short-range forces and will be affected by the details of the surface region. Beyond this distance, which need not be further specified here, Eq. (A-8) will be valid. If an external field,  $E$ , is now applied to the metal, the potential outside the metal is given by (Fig. A-3):

$$\Phi(x) = \frac{e}{16\pi\epsilon_0 x} + Ex + \text{constant} \quad (\text{A-9})$$

This potential function has a minimum at

$$x_s = \frac{1}{4} \sqrt{\frac{e}{\epsilon_0 E}} \quad (\text{A-10})$$

The difference between the potential (Eq. A-9) at  $x_s$  and the potential at infinity in the absence of the applied field represents a lowering of the potential barrier for electron emission. The work function in the presence of an applied field is (remembering to multiply the potential by the electronic charge to yield an energy)

$$\phi = \phi_0 - \frac{e^{3/2} \sqrt{E}}{\sqrt{4\pi\epsilon_0}} \quad (\text{A-11a})$$

$$\phi = \phi_0 - 3.79 \times 10^{-5} \sqrt{E} \quad (\text{A-11b})$$

where  $\phi_0$  is the initial work function (in electron volts) in the absence of a field, and  $E$  is the applied electric field (in volts per meter).

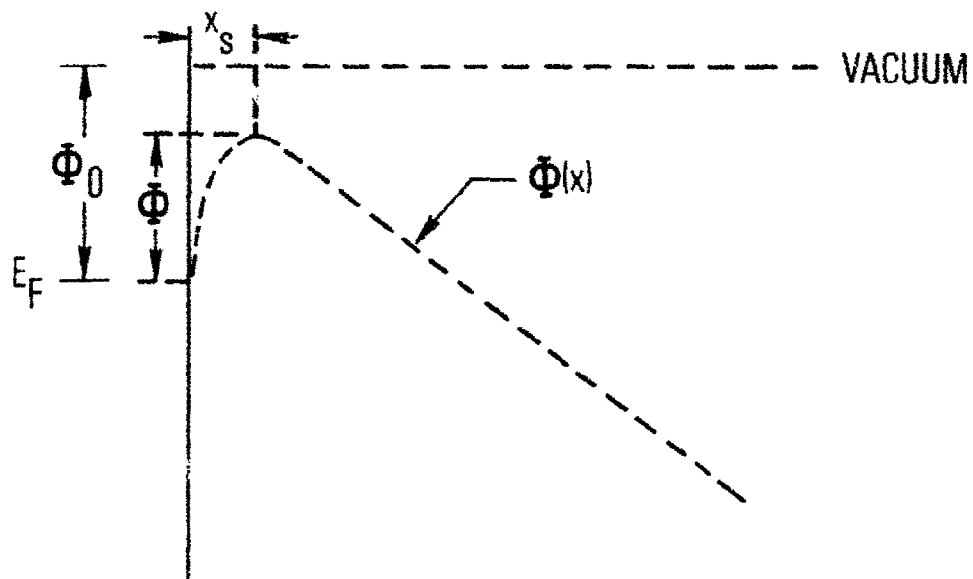


Fig. A-3. Electrostatic Potential as Function of Distance from Surface in Presence of Externally Applied Electric Field.

#### 4. RETARDING-FIELD REGION

If the anode is biased negatively by a potential  $V_A$ , an additional potential barrier must be overcome by the emitted electrons in the diode configuration of Fig. 2. Strictly speaking, the additional barrier is  $-eV_A + \phi_A - \phi_C$ , where  $V_A < 0$ , and  $\phi_A$  and  $\phi_C$  are the anode and cathode work functions, respectively. The current density is

$$J = J_0 \exp\left(\frac{eV_A - \phi_A + \phi_C}{kT}\right) \quad (\text{A-12})$$

where  $J_0$  is given by the Richardson-Dushman equation, Eq. (A-3).

In summary, a plot of current versus applied voltage in a diode configuration, a standard test configuration, can be divided into distinct regions of operation: (1) the retarding-field region; (2) the space-charge-limited region (Langmuir-Child law); (3) the saturation current region (Richardson-Dushman equation); and (4) at sufficiently high applied fields, the Shottky reaction. These operating regions are encountered, in the order given, as the anode voltage is made more positive and, in general, are observed for emitters other than metals as well. Note that in the intermediate-field region the Richardson-Dushman equation predicts the number of electrons that could be emitted from a cathode at a given temperature. The Langmuir-Child law yields the number of electrons that are emitted and actually reach the anode. Most vacuum tubes, including all space TWTs, operate in the space-charge-limited region. The space-charge cloud serves as a "fly wheel" to stabilize tube operation. Small variations in cathode temperature should not, at least in principle, have a significant effect on tube current.

#### B. THERMIONIC EMISSION FROM SEMICONDUCTORS

In the discussion of the Richardson-Dushman equation, care was taken to point out that the result is general. If the thermodynamic derivation is considered, it is clear that nowhere in the derivation is it assumed that the

emitter is a metal. Note also that the density of conduction electrons does not enter directly into the Richardson-Dushman equation. Most of the conduction electrons cannot contribute to thermionic emission because of the exclusion principle. Only the occupation of energy states above the nearly completely occupied states of the conduction band is of concern.

It does seem, intuitively, that the density of conduction electrons should be important in thermionic emission. Observation of thermionic emission from an insulator is not expected if only because the low electrical conductivity would prevent electrons from the power source from replacing emitted electrons without excessive voltage drop. The answer to the question raised here is that the conduction electron density does enter the Richardson-Dushman equation indirectly through its effect on the work function.

It is possible to make a number of general observations pertinent to thermionic emission from nonmetals. These generalizations do not seem to have been explicitly stated in the literature. In a semiconductor, it is customary to refer energies to the bottom of the conduction band and to introduce the electron affinity  $\chi$ , defined as the energy interval between the bottom of the conduction band and the vacuum level.

The work function of a semiconductor (Fig. A-1b) is then

$$\phi = -E_F + \chi, \quad (\text{A-13})$$

i. e., the interval between the Fermi level and the vacuum level, just as in the case of a metal. The electron affinity for semiconductors with primarily covalent bonding is on the order of 3.5 to 4.5 eV.<sup>7</sup> Electron affinities in ionic materials have not been as extensively measured; however, in BaO, for example, the electron affinity is 0.7 to 1.0 eV.<sup>8</sup> It is expected that electron affinity should be generally lower in ionic than in covalent materials. In an ionic compound, atomic shells are, to first approximation,

completely filled. An electron added to an ionic material has no conveniently available orbitals in which it can be accommodated. Its binding energy, i. e., the electron affinity, is low. In a covalent material, orbitals are more readily available since the electron distribution about constituent atoms is not completely spherically symmetric. Electrons might, for example, be placed in d-orbitals. Electron affinity thus would be higher than in an ionic compound.

These considerations imply that any search for better semiconducting thermionic emitters should concentrate on ionic materials, or at least on materials not strongly covalent. Even with heavy doping, the Fermi level in a semiconductor cannot be moved far up into the conduction band, and the work function is at least as large as the electron affinity. Studies of fairly covalent materials, e. g., various uranium compounds,<sup>9</sup> confirm that these materials do have higher work functions than are found for conventional oxide cathodes (they were investigated for use in thermionic energy conversion devices and were to be fission heated in a neutron flux).

These general observations may be made more quantitative. An intrinsic semiconductor (an insulator is an intrinsic semiconductor with a large bandgap) is considered. The Fermi level is related to the temperature by the expression<sup>10</sup>

$$E_F = -\frac{1}{2} E_g + \frac{3}{4} kT \ln \left( \frac{m_h}{m_e} \right) \quad (\text{A-14})$$

The width of the energy gap is  $E_g$ ; the effective masses of holes and electrons are given by  $m_h$  and  $m_e$ , respectively. The zero of energy is taken to be the bottom of the conduction band. If Equations (A-13) and (A-14) are substituted in Eq. (A-3c),

$$J = A(1 - \bar{r}) \left( \frac{m_e}{m_h} \right)^{3/4} \exp - \frac{E_g/2 + \chi}{kT} \quad (\text{A-15})$$

The quantity  $E_g/2 + \chi$  is large for an insulator or wide-band gap semiconductor, and the thermionic emission current attainable at temperatures below the melting point is insignificant, which is in agreement with intuition. For silicon at its melting point,  $J = 280 \text{ nA/cm}^2$ .

Practical semiconductor cathodes are impurity materials and, since "holes" cannot be emitted, must be n-type. The energy level diagram of a semiconductor emitter (BaO) is illustrated in Fig. 1. The donor levels are located in the energy gap just below the conduction band. An expression for the position of the Fermi level is readily found in standard reference works on solid-state physics<sup>1</sup>

$$E_F = -\frac{E_d}{2} + \frac{kT}{2} \ln \left[ n_d \frac{h^3}{2(2\pi mkT)^{3/2}} \right] \quad (\text{A-16})$$

where  $E_d$  is the energy of the donor level. All energies are measured relative to the bottom of the conduction band. Substitution of the above expression in Eq. (A-3) yields

$$J = (1 - \bar{r}) n_d^{1/2} \frac{\sqrt{2} e (2\pi m)^{1/4}}{h^{3/2}} k^{5/4} t^{5/4} \exp \left( -\frac{E_d/2 + \chi}{kT} \right) \quad (\text{A-17})$$

It is satisfying that this emission expression, known as the Fowler equation, does depend explicitly on the density of electron donors. Certain complications limit the application of the Fowler equation. The validity of Eq. (A-16) and therefore Eq. (A-17) is limited to temperatures below the range of operation of practical cathodes.  $\chi$  is also a function of temperature. Equation (A-17) however, is useful as a guide to more refined cathode models.

## APPENDIX A

### REFERENCES

1. C. Kittel, Introduction Solid State Physics, 3rd ed., John Wiley and Sons, New York (1966).
2. A. K. Vijn and P. Lenfant, Canadian J. Phys. 51, 111 (1973).
3. C. Herring and M. H. Nichols, Rev. Mod. Phys. 21, 185 (1949).
4. G. A. Haas and R. E. Thomas, "Thermionic Emission and Work Function," in Techniques of Metals Research, E. Passaglia, ed., Interscience, New York (1972).
5. W. B. Nottingham, Thermionic Emission, Report No. 321, MIT Research Laboratory of Electronics (10 December 1956).
6. A. Venema, "Thermionic Emission," in Handbook of Vacuum Physics, Vol. II, Chapt. 2, A. H. Beck, ed., Pergammon Press (1966).
7. D. L. Feucht and A. G. Milnes, Heterojunction and Metal-Semiconductor Junctions, Academic Press, New York (1972).
8. L. S. Nergaard, RCA Rev. 13, 464 (1952).
9. G. A. Haas and J. T. Jensen, J. Appl. Phys. 34, 3451 (1963).

## APPENDIX B

### WORK FUNCTION

#### A. WORK FUNCTION OF METALS

The work function has so far been simply accepted as a given quantity for a metal. An understanding of work function variation among different metals and among different crystal faces of a particular metal is required in order to understand thermionic emission (Fig. B-1a). The electron distribution of a metal will spread beyond the outermost layer of surface atoms. The boundary between the interior and the exterior of the metal cannot be completely abrupt since such a boundary would require rapidly changing wave functions representing electrons of high kinetic energy.<sup>1</sup> By the spreading of the electron distribution outside the metal, the kinetic energy of the electrons is reduced. The potential energy of the electrons, however, will be increased. At equilibrium, the situation shown in Fig. B-1b will prevail. This configuration represents a separation of positive and negative charge (Fig. B-1c) and causes a surface dipole moment.

The removal of an electron from the metal is considered next. The work function is defined as the change in (Helmholtz) free energy of the metal when an electron at the Fermi level is removed, at constant temperature and volume, to a position at rest at infinity. It is convenient to divide the energy required into a bulk term, which represents the energy change if the electron distribution around the surface atoms were the same as for bulk atoms, and a surface term representing the energy change as a result of the surface dipole moment  $D$ .

$$\phi = \left. \frac{\partial F}{\partial N} \right|_{T, V} + \frac{eD}{\epsilon_0} \quad (\text{B-1})$$

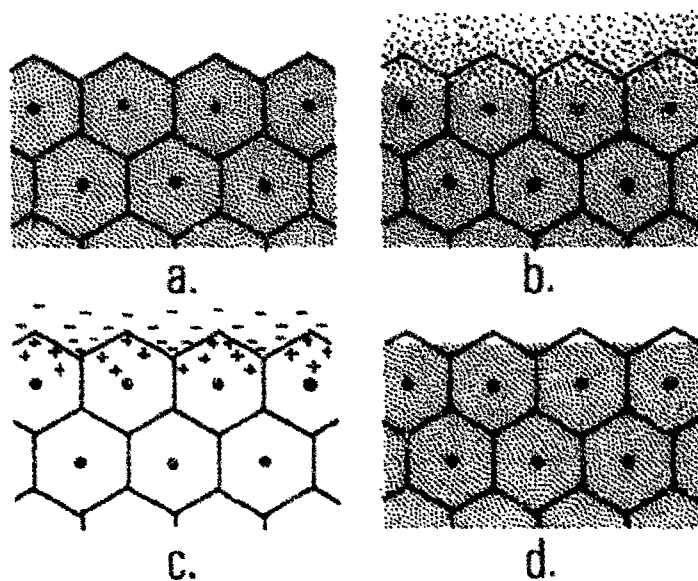


Fig. B-1. Electron Double Layer Formation at Metal Surface as Result of Spreading of the Electron Distribution. a. Charge distribution if distribution of electrons about surface atoms were same as in bulk. b. Actual charge distribution near metal surface is represented by density of stippling. Electrons are found outside of volume that alone would be occupied if surface atom electron distribution were identical to that in bulk. c. "Leakage" of electrons beyond idealized surface of Fig. 1a results in charge distribution equivalent to dipole layer, with negative side outermost, superimposed on idealized distribution. Difference between charge distributions of Figs. B-1a and B-1b. d. Characteristic wavelength of electrons in metal is large compared to dimensions of surface features. Electron distribution thus tends to be smoother than surface geometry.

where  $F$  is the free energy, and  $N$  is the number of electrons in the metal.<sup>2</sup> The term  $\partial F/\partial N$  is the chemical potential and, in fact, is, by definition, the Fermi energy.

The bulk ( $\partial F/\partial N$ ) contribution to the work function can be handled reasonably well theoretically. At  $T = 0$  K,  $\partial F/\partial N$  can be replaced by  $\partial E/\partial N$ , where  $E$  is the cohesive energy. Calculations of cohesive energy have been made by Wigner and Wigner and Bardeen, among others.<sup>3,4</sup> These theories yield  $E(N)$ . The calculation of the surface dipole moment is more difficult. The dipole contribution is estimated by subtracting the calculated bulk term from the measured value of the work function. The surface dipole moment can be very substantial, ranging from a few tenths of an electron volt up to several electron volts. More recently, the Fermi-Thomas model was applied rather successfully to the calculation of work functions.<sup>5</sup> Both the bulk and surface terms are given by the Fermi-Thomas model in terms of the lattice constant and one parameter. Agreement with experiment is satisfactory (about  $\pm 10\%$ ) for those metals to which the model is applicable. The theory is not applicable to metals in which the diameter of the ion cores is comparable to the lattice spacing, e. g., copper, silver, and zinc. The theory, furthermore, does not permit calculation of differences in work function between crystallographic surface planes of the same metal.

It has been pointed out that the spreading of electrons beyond the outermost atomic layer results in a surface dipole moment. The actual electron distribution represents a compromise between potential and kinetic energy. If a surface is not flat, but contains ridges and valleys, the electronic potential energy is minimized if the electrons preferentially bunch up in the ridges. This bunching increases electron kinetic energy (higher frequency Fourier components are required to describe the electron distribution), and the electron distribution on a rough surface will be

smoother than the surface topography if the spacing between the peaks and valleys is on the order of atomic dimensions. The smoothing is equivalent to an additional contribution to the surface dipole moment with the positive end outward. The smoothing is more pronounced with rougher surfaces, which accounts for the fact that the work function is highest on the most atomically smooth surfaces.

Many attempts to relate the work function to various bulk atomic properties have been reported, e. g., to electronegativity,<sup>6</sup> ionization energy,<sup>7</sup> and to atomic radii<sup>8</sup> (these quantities are related). Such theories are intrinsically incapable of yielding the dipole contribution to the work function and, therefore, cannot account for work function differences between different crystallographic planes.

A semiempirical theory by Steiner and Gytopoulos does, however, predict work functions and their crystallographic variation reasonably well. The method is based on an expression for atomic electronegativity that explicitly includes the coordination number of surface atoms. Details are given in Ref. 9.

In summary, whereas work function calculations have been carried out for many metals with reasonable agreement with experiment, ab initio calculations are not sufficiently accurate to account in detail for work function differences between crystallographic planes. The qualitative nature of these differences is understood and semiempirical theories are available. Note that detailed calculations of work functions for different metals and for different crystal planes of a given metal probably would not have much importance in the construction of practical cathodes. The qualitative prediction of trends, which can be accomplished, is of greater importance.

## B. WORK FUNCTION OF MONOLAYER SYSTEMS

Monolayer adsorption of electropositive species on metals has been extensively studied. Since these systems constitute perhaps the simplest

possible examples of chemisorption, they have been a favorite research subject for both experimental and theoretical scientists, quite apart from any considerations of application to cathode development.

A single electropositive atom, i. e., an alkali metal or alkaline earth element, is considered to be adsorbed on a metal surface with a high work function, e. g., tungsten. If the work function of the substrate exceeds the ionization potential of the atom, then the adatom should ionize. The ionized surface atom, together with its classical image charge, form a dipole. For a surface layer of (widely separated) adatoms, the potential change at the surface as a result of the dipoles formed is

$$\Delta\Phi = \frac{n}{\epsilon_0} qd \text{ (MKS units)} \quad (\text{B-2})$$

where  $n$  is the number of adatoms per square centimeter,  $q$  the ionic charge ( $q = e$  for a completely ionized, univalent atom), and  $d$  the dipole spacing ( $d = 2r$ , where  $r$  is the ionic radius and is the distance between the charge center of the ion and its image charge).  $\Delta\Phi$  is an electrostatic potential change expressed in volts. With the convention adopted in Section IV. B, the corresponding energy change for an electron is denoted by  $\Delta\phi$ . These quantities are numerically equal if energies are expressed in units of electron volts. For a complete surface monolayer ( $n \approx 10^{15}/\text{cm}^2$ ) with  $d \approx 4 \text{ \AA}$  and  $q = e$ ,  $\Delta\phi = 73 \text{ eV}$ . This value is too large to be physically reasonable. If measured values of  $\phi$  versus surface coverage  $n$  for various alkali or alkaline earth atoms adsorbed on metal substrates are plotted, the behavior illustrated in Fig. B-2 is found. At first,  $d\phi/dn$  is comparable to the value expected from Eq. (B-2), then decreases in magnitude.  $\phi(n)$  goes through a minimum, then increases slightly to nearly equal the bulk work function of the adsorbed species at about one monolayer coverage. Since the minimum value of  $\phi(n)$  is actually less than the bulk work function of the adsorbed species, Fig. B-2 indicates that a practical thermionic emitter based on the surface dipole moment of a surface monolayer could be constructed. Such cathodes are in fact in wide use.

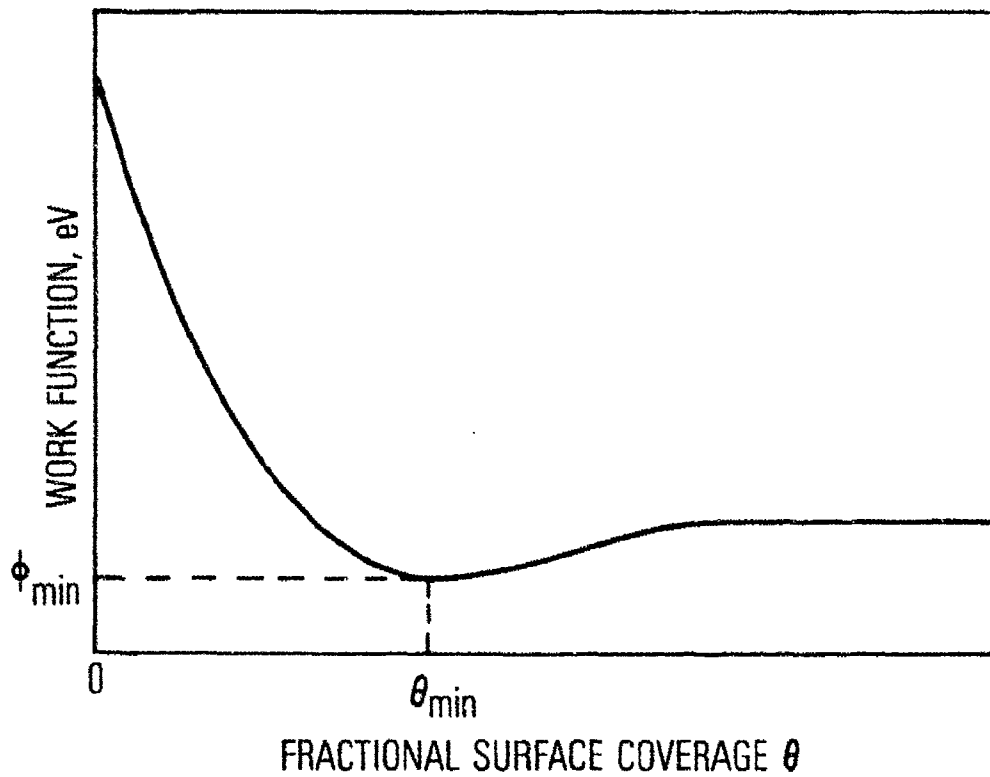


Fig. B-2. General Behavior of Work Function as Function of Surface Coverage for Alkali or Alkaline Earth Element Adsorbed on Metal Substrate

The observed work function minimum is well understood, at least qualitatively.<sup>10</sup> The point is that as the adatom surface density  $n$  increases, interaction of adatoms results in a decrease in the charge per atom,  $q$ . Equation (B-2) therefore exhibits a minimum. Early discussions of the problem employed depolarization models in which the field of each surface dipole contributed to a reduction in the moment of other surface dipoles.<sup>11</sup> More complete and recent models are firmly based on quantum mechanics.<sup>12, 13</sup> As an alkali metal atom approaches a surface to a distance  $d$ , the adatom energy levels are raised by  $e^2/4\pi\epsilon_0 d$  (Fig. B-3). The alkali  $ns$  level, which lies above the Fermi level, is also broadened, with a tail extending below the Fermi level. In other words, the adatom is partially ionized ( $q < e$ ). As adatom coverage increases, the alkali level is lowered, and the adatom layer is gradually neutralized. A complete adatom monolayer is essentially neutral and metallic. Work function changes in the limit of complete monolayer coverage also have been treated theoretically.<sup>14, 15</sup>

Experimental studies of the adsorption of alkali and alkaline earth species on metal substrates are too numerous to list in detail in this report. Cesium and barium have been favorite adsorbates, whereas tungsten has been a favorite adsorbent. Work also has been carried out with nickel substrates.<sup>16-20</sup> Experiments with these materials are particularly relevant to cathode technology. Low-energy electron diffraction has been widely used to determine the structure of adsorbed monolayers, whereas work function measurements generally have been carried out by means of either field emission or the contact potential difference technique. The  $\phi(n)$  behavior illustrated in Fig. B-2 is found quite generally. Coadsorption of two electropositive species has also been investigated.<sup>21</sup>

Coadsorption of an electropositive species with oxygen on metal substrates, e. g., sodium on oxygen-covered tungsten (Na-O-W),<sup>10</sup> Cs-O-W,<sup>10, 22</sup> Ba-O-W,<sup>23</sup> BaO-W,<sup>24</sup> and Cs-O-Ni,<sup>10, 25, 26</sup> has been

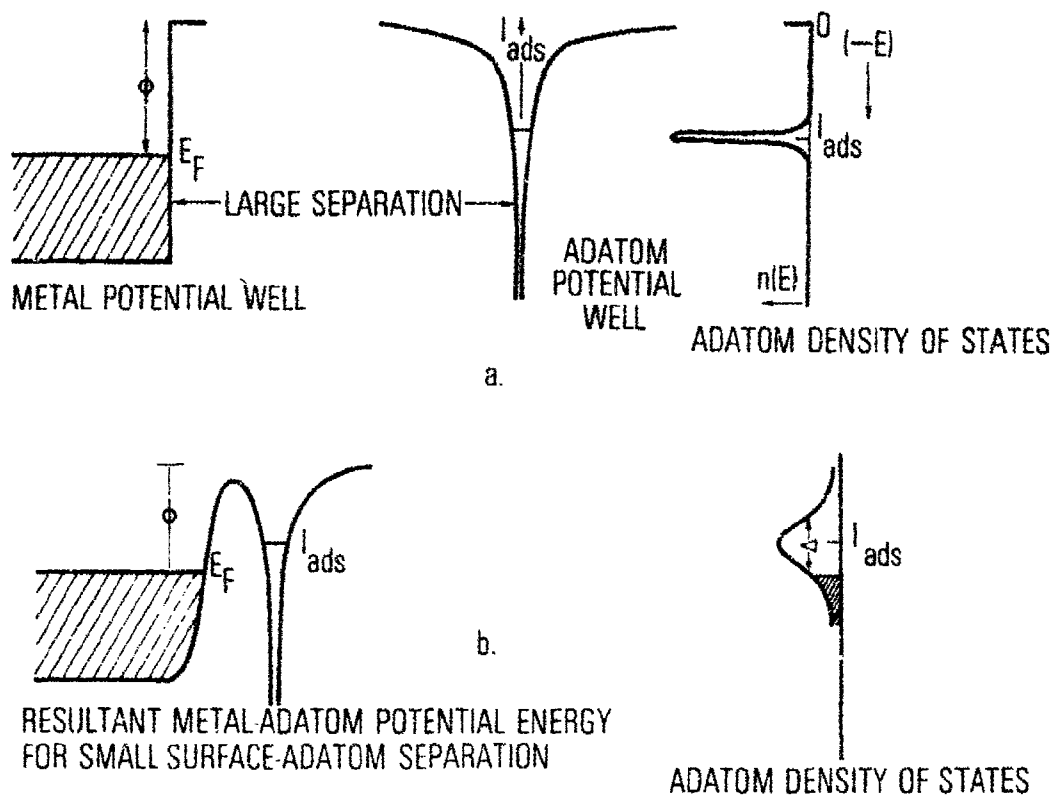


Fig. B-3. Potential Energy Diagrams. a. Metal and ionizable donor species, wide separation. (The density of the states of the atom, also shown, is a sharply peaked function.) b. Metal and ionizable donor species at small separation. (Note that the adatom density of states is broadened.)

investigated. In all of these experiments, low-energy electron diffraction, generally in conjunction with work function measurements, was employed. The result most pertinent to cathode technology is that a double layer is formed with the alkali or alkaline earth above the oxygen regardless of the order of adsorption.<sup>10</sup> The same general behavior of  $\phi(n)$  illustrated in Fig. B-2 is observed with the alkali (alkaline earth)-oxygen-substrate system, and the minimum work function is generally lower than in the absence of oxygen. For example, with Cs-O-W (112) [or O-Cs-W (112)]  $\phi_{\min} \approx 1.1$  eV,<sup>10</sup> while  $\phi_{\min} \approx 1.55$  eV for Cs-W (112).<sup>16</sup>

APPENDIX B

REFERENCES

1. C. Herring, "The Atomistic Theory of Atomic Surfaces," in Metal Interfaces, ASTM, Cleveland (1952).
2. C. Herring and M. H. Nichols, Rev. Mod. Phys. 21, 185 (1949).
3. E. Wigner, Phys. Rev. 46, 1002 (1934).
4. E. Wigner and J. Bardeen, Phys. Rev. 48, 84 (1935).
5. B. F. Rzyanin, High Temp. 11, (1973) (English translation).
6. W. Gordy and W. J. O. Thomas, Phys. Rev. 24, 439 (1956).
7. C. F. Gallo and W. L. Lama, IEEE Trans. Ind. Appl. 1A 10, 496 (1974).
8. R. O. Jenkins, Vacuum 19, 353 (1969).
9. G. A. Haas and R. E. Thomas, "Thermionic Emission and Work Function," in Techniques of Metals Research, Vol. 6, Part 1, E. Passaglia, ed., Interscience, New York (1972).
10. J. M. Chen, J. Franklin Inst., 298, 255 (1974).
11. I. Langmuir, J. Am. Chem. Soc. 54, 2798 (1932).
12. J. W. Gadzuk, J. K. Hartman, and T. N. Rhodin, Phys. Rev. B 4, 241 (1971).
13. J. P. Muscat and D. M. Newns, J. Phys. C. 7, 2630 (1974).
14. N. D. Lang, Phys. Rev. B 4, 4234 (1971).
15. K. F. Wojciechowski, Surface Sci. 55, 246 (1976).
16. V. M. Gavriilyuk, A. G. Naumovets, and A. G. Fedorus, Sov. Phys. JETP 24, 899 (1967).
17. A. G. Fedorus, Yu. M. Konoplev, and A. G. Naumovets, Sov. Phys. Solid State 11, 160 (1969).

18. V. K. Medvedev and T. P. Smerka, Sov. Phys. Solid State 15, 507 (1973).
19. D. A. Gordetsky and Yu. P. Melneck, Surface Sci. 62, 647 (1977).
20. V. K. Medvedev and A. I. Yakivchuk, Sov. Phys. Solid State 17, 7 (1975).
21. Yu. M. Konoplev, A. G. Naumovets, and A. G. Fedorus, Sov. Phys. Solid State 14, 273 (1972).
22. C. A. Papageorgopoulos and J. M. Chen, J. Vacuum Sci. and Technol. 9, 570 (1972).
23. Yu. S. Vedula, V. M. Gavriilyuk, and N. D. Morgulis, Sov. Phys. Solid State 1, 1569 (1960).
24. B. J. Hopkins and K. J. Ross, Brit. J. Appl. Phys. 16, 1319 (1965).
25. C. A. Papageorgopoulos and J. M. Chen, Solid State Communications 13, 1455 (1973).
26. C. A. Papageorgopoulos and J. M. Chen, Surface Sci. 52, 40 (1975).

## LABORATORY OPERATIONS

The Laboratory Operations of The Aerospace Corporation is conducting experimental and theoretical investigations necessary for the evaluation and application of scientific advances to new military concepts and systems. Versatility and flexibility have been developed to a high degree by the laboratory personnel in dealing with the many problems encountered in the Nation's rapidly developing space systems. Expertise in the latest scientific developments is vital to the accomplishment of tasks related to these problems. The laboratories that contribute to this research are:

Aerophysics Laboratory: Aerodynamics; fluid dynamics; plasmadynamics; chemical kinetics; engineering mechanics; flight dynamics; heat transfer; high-power gas lasers, continuous and pulsed, IR, visible, UV; laser physics; laser resonator optics; laser effects and countermeasures.

Chemistry and Physics Laboratory: Atmospheric reactions and optical backgrounds; radiative transfer and atmospheric transmission; thermal and state-specific reaction rates in rocket plumes; chemical thermodynamics and propulsion chemistry; laser isotope separation; chemistry and physics of particles; space environmental and contamination effects on spacecraft materials; lubrication; surface chemistry of insulators and conductors; cathode materials; sensor materials and sensor optics; applied laser spectroscopy; atomic frequency standards; pollution and toxic materials monitoring.

Electronics Research Laboratory: Electromagnetic theory and propagation phenomena; microwave and semiconductor devices and integrated circuits; quantum electronics, lasers, and electro-optics; communication sciences, applied electronics, superconducting and electronic device physics; millimeter-wave and far-infrared technology.

Materials Sciences Laboratory: Development of new materials; composite materials; graphite and ceramics; polymeric materials; weapons effects and hardened materials; materials for electronic devices; dimensionally stable materials; chemical and structural analyses; stress corrosion; fatigue of metals.

Space Sciences Laboratory: Atmospheric and ionospheric physics, radiation from the atmosphere, density and composition of the atmosphere, aurorae and airglow; magnetospheric physics, cosmic rays, generation and propagation of plasma waves in the magnetosphere; solar physics, x-ray astronomy; the effects of nuclear explosions, magnetic storms, and solar activity on the earth's atmosphere, ionosphere, and magnetosphere; the effects of optical, electromagnetic, and particulate radiations in space on space systems.